

## RESEARCH ARTICLE

# NIK–IKK complex interaction controls NF- $\kappa$ B-dependent inflammatory activation of endothelium in response to LT $\beta$ R ligation

Paulina Kucharzewska<sup>1,\*,\$</sup>, Chrissta X. Maracle<sup>2,‡</sup>, Kim C. M. Jeucken<sup>2,‡</sup>, Jan Piet van Hamburg<sup>2</sup>, Elisabeth Israelsson<sup>1</sup>, Mark Furber<sup>1</sup>, Sander W. Tas<sup>2</sup> and Henric K. Olsson<sup>1</sup>

**ABSTRACT**

NF- $\kappa$ B-inducing kinase (NIK; also known as MAP3K14) is a central regulator of non-canonical NF- $\kappa$ B signaling in response to stimulation of TNF receptor superfamily members, such as the lymphotoxin- $\beta$  receptor (LT $\beta$ R), and is implicated in pathological angiogenesis associated with chronic inflammation and cancer. Here, we identify a previously unrecognized role of the LT $\beta$ R–NIK axis during inflammatory activation of human endothelial cells (ECs). Engagement of LT $\beta$ R-triggered canonical and non-canonical NF- $\kappa$ B signaling promoted expression of inflammatory mediators and adhesion molecules, and increased immune cell adhesion to ECs. Sustained LT $\beta$ R-induced inflammatory activation of ECs was NIK dependent, but independent of p100, indicating that the non-canonical arm of NF- $\kappa$ B is not involved. Instead, prolonged activation of canonical NF- $\kappa$ B signaling, through the interaction of NIK with I $\kappa$ B kinase  $\alpha$  and  $\beta$  (also known as CHUK and IKBKB, respectively), was required for the inflammatory response. Endothelial inflammatory activation induced by synovial fluid from rheumatoid arthritis patients was significantly reduced by NIK knockdown, suggesting that NIK-mediated alternative activation of canonical NF- $\kappa$ B signaling is a key driver of pathological inflammatory activation of ECs. Targeting NIK could thus provide a novel approach for treating chronic inflammatory diseases.

**KEY WORDS:** NF- $\kappa$ B-inducing kinase, NIK, Lymphotoxin- $\beta$  receptor, LT $\beta$ R, Inflammation, Endothelial cells

**INTRODUCTION**

Vascular endothelial cells (ECs) are crucial participants and regulators of normal immune and inflammatory responses (Pober and Sessa, 2007), and endothelial dysfunction may play a central role in the pathogenesis of chronic inflammatory diseases, e.g. rheumatoid arthritis (RA) (Murdaca et al., 2012; Noort et al., 2015a; Steyers and Miller, 2014; Al-Soudi et al., 2017). As a driver of chronic inflammation in RA, endothelial dysfunction involves pathological responses of ECs, such as inflammatory activation, angiogenesis,

high endothelial venule (HEV) differentiation and tertiary lymphoid organ (TLO) formation. Upon inflammatory activation, ECs express adhesion molecules and produce chemokines, thereby recruiting immune cells into the synovial tissue (Murdaca et al., 2012; Steyers and Miller, 2014; Al-Soudi et al., 2017). Angiogenesis is driven by activated stromal and inflammatory cells secreting angiogenic factors, e.g. VEGFA, that trigger quiescent ECs to differentiate and form new blood vessels, which contribute to persistent inflammation (Elshabrawy et al., 2015). TLOs are formed in a process of lymphoid neogenesis, involving conversion of chronic inflammatory infiltrates into organized lymphoid tissue with HEV and sometimes even true germinal centers. These aggregates seem to facilitate the process of epitope spreading associated with autoimmunity and may exacerbate inflammation (Humby et al., 2009; Pitzalis et al., 2014; Noort et al., 2015a; Jones and Jones, 2016). Given the central role of endothelial dysfunction in the pathophysiology of inflammatory diseases, signaling pathways that control EC activation have been extensively studied, and the NF- $\kappa$ B family of transcription factors has been identified as critical for expression of many of the genes associated with EC pathology (Pober and Sessa, 2007; Tas et al., 2016).

The nuclear factor- $\kappa$ B (NF- $\kappa$ B) transcription factors operate as heterodimers with a predominance for pairing of p50 (also known as NFKB1)/p65 (also known as RELA), p50/c-Rel and p52 (also known as NFKB2)/RelB (Hayden and Ghosh, 2004; Napetschnig and Wu, 2013). Activation of canonical NF- $\kappa$ B signaling in response to pro-inflammatory stimuli, such as TLR ligands, IL-1 $\beta$  and TNF $\alpha$  (also known as TNF) leads to ubiquitin-dependent degradation of I $\kappa$ B $\alpha$  (also known as NFKBIA), and, as a consequence, nuclear translocation of NF- $\kappa$ B complexes, especially p50/p65 heterodimers. Degradation of I $\kappa$ B $\alpha$  is triggered by its phosphorylation by the trimeric I $\kappa$ B kinase (IKK) complex, which is composed of two catalytic subunits, IKK $\alpha$  (also known as CHUK) and IKK $\beta$  (also known as IKBKB), and a regulatory subunit, IKK $\gamma$  [also known as NF- $\kappa$ B essential modulator (NEMO) or IKBKG] (Hayden and Ghosh, 2004; Napetschnig and Wu, 2013). In contrast, the non-canonical NF- $\kappa$ B pathway is strictly dependent on NF- $\kappa$ B-inducing kinase (NIK; also known as MAP3K14), which activates IKK $\alpha$  to phosphorylate the p100/NF- $\kappa$ B2 precursor protein, leading to its processing to p52 (Napetschnig and Wu, 2013; Sun, 2017), followed by nuclear translocation of p52:RelB heterodimers and, ultimately, target gene transcription (Bonizzi et al., 2004; Lovas et al., 2008; Madge et al., 2008; Kew et al., 2012). This pathway is activated via TNF receptor superfamily members, such as the lymphotoxin- $\beta$  receptor (LT $\beta$ R), B-cell-activating factor receptor (BAFFR; also known as TNFRSF13C) and CD40. All known inducers of the non-canonical NF- $\kappa$ B pathway can also activate canonical NF- $\kappa$ B signaling, but to

<sup>1</sup>Respiratory, Inflammation and Autoimmunity IMED Biotech Unit, AstraZeneca, Gothenburg, SE-431 83 Mölndal, Sweden. <sup>2</sup>Amsterdam Rheumatology and Immunology Center, Department of Clinical Immunology and Rheumatology and Laboratory for Experimental Immunology, Academic Medical Center/University of Amsterdam, 1105 AZ Amsterdam, The Netherlands.

\*Present address: Department of Physiological Sciences, Faculty of Veterinary Medicine, Warsaw University of Life Sciences, 02-787 Warsaw, Poland.

<sup>‡</sup>These authors contributed equally to this work

<sup>\$</sup>Author for correspondence (paulina\_kucharzewska\_siembieda@sggw.pl)

 P.K., 0000-0002-4698-2551

what extent may vary between stimuli (Napetschnig and Wu, 2013; Sun, 2017).

Whereas the role of canonical NF- $\kappa$ B signaling in inflammatory activation of ECs and angiogenesis is well established (De Martin et al., 2000; Huang et al., 2000; Kempe et al., 2005; Pober and Sessa, 2007; Tas et al., 2016), the function of non-canonical NF- $\kappa$ B signaling in ECs, especially in the context of inflammation, is less defined. Previous studies have shown that ECs express LT $\beta$ R and CD40, and that the ligation of LT $\beta$ R results in expression of CXCL12 in a non-canonical NF- $\kappa$ B-dependent manner (Hollenbaugh et al., 1995; Chang et al., 2005; Madge et al., 2008). Recently, it was demonstrated that LT $\beta$ R signaling in ECs is crucial for the development and function of HEVs and lymph node homing of lymphocytes (Onder et al., 2013). Interestingly, NIK-positive HEVs are also present at sites of chronic inflammation, such as RA synovial tissue, indicating that NIK and the non-canonical NF- $\kappa$ B pathway may regulate TLO formation downstream of LT $\beta$ R in chronic inflammation by regulating the development of the cuboidal HEV-like appearance and functions, including the acquisition of leukocyte traffic-regulating properties (Noort et al., 2015a). Additionally, NIK is activated in blood vessels of tumor tissues and inflamed RA synovial tissue, and promotes pathological angiogenesis in response to LT $\beta$ R or CD40 ligation (Noort et al., 2014; Maracle et al., 2017). Furthermore, NIK expression in the blood vessels in the synovium of early RA patients is positively correlated with inflammatory cell infiltration and disease activity, as measured by joint swelling, erythrocyte sedimentation rate and C-reactive protein levels (Maijer et al., 2015), suggesting that, in addition to regulating pathological angiogenesis, NIK may also modulate the inflammatory phenotype of endothelium. However, the role of NIK and downstream NF- $\kappa$ B signaling during the inflammatory activation of ECs remains elusive. Improved molecular understanding of this pathway is needed to provide more insight into the pathogenesis of chronic inflammation, and, in this study, we identify NIK as a key mediator of inflammatory activation of ECs in response to LT $\beta$ R ligation.

## RESULTS

### LT $\beta$ R ligation activates canonical and non-canonical NF- $\kappa$ B signaling pathways and induces inflammation in ECs

To confirm LT $\beta$ R-induced NF- $\kappa$ B signaling in ECs (Dejardin et al., 2002; Müller and Siebenlist, 2003; Madge et al., 2008; Wolf et al., 2010; Lau et al., 2014), we probed for non-canonical and canonical NF- $\kappa$ B activation in human umbilical vein ECs (HUVECs) stimulated with lymphotoxin  $\alpha$ 1/ $\beta$ 2 (LT $\beta$ ) or LIGHT (also known as TNFSF14). Both LT $\beta$  and LIGHT induced strong and dose-dependent activation of non-canonical NF- $\kappa$ B signaling in HUVECs, as shown by increased levels of NIK and p52 protein, the processed (activated) form of p100 protein (Fig. 1A; Fig. S1A). Activation of non-canonical NF- $\kappa$ B signaling in response to LT $\beta$ R ligation was slow (i.e. only apparent after several hours) but long lasting (at least 48 h) (Fig. 1A). LT $\beta$  and LIGHT also induced classical NF- $\kappa$ B signaling in HUVECs (Fig. 1B); however, in contrast to non-canonical NF- $\kappa$ B signaling, the canonical pathway was activated within minutes by both cytokines, inducing I $\kappa$ B $\alpha$  degradation, with levels reaching a minimum at 30 min of stimulation and returning to baseline within 1 h of stimulation. LT $\beta$ R ligation induced activation of the two NF- $\kappa$ B signaling pathways in a similar manner in the human vascular EC line EA.hy926 (Fig. S1B–D) and in human microvascular ECs (HMVECs) (Fig. S1F,G).

LT $\beta$ R-induced nuclear accumulation of NF- $\kappa$ B proteins in HUVECs followed similar pathway activation kinetics, with

maximal nuclear localization of classical NF- $\kappa$ B proteins (p50 and p65) observed at 2 h of stimulation with LT $\beta$  and LIGHT, whereas nuclear accumulation of the non-canonical NF- $\kappa$ B proteins (RelB and p52) was much slower, requiring >8 h to reach maximal levels (Fig. 1C; Fig. S2A). We did not observe any substantial effect of LT $\beta$ R ligation on nuclear localization of c-Rel (Fig. 1C).

NF- $\kappa$ B signaling is a key regulator of inflammatory responses, and, to assess the potential impact of LT $\beta$ R-induced NF- $\kappa$ B activity on inflammatory activation of endothelium, we stimulated ECs with either LT $\beta$  or LIGHT and analyzed expression of NF- $\kappa$ B target genes. Both stimuli induced the expression of inflammatory cytokines and chemokines [CXCL1, CXCL5, CXCL8, GM-CSF (also known as CSF2), CCL2, CCL5, CCL20], as well as adhesion molecules mediating immune cell recruitment (ICAM-1, VCAM-1 and E-selectin), both at mRNA (Fig. 1D) and protein levels (Fig. 1E,F; Fig. S1I). Furthermore, LT $\beta$ R ligation induced an increase in endothelial barrier permeability (Fig. 1G) and adhesion of Jurkat T cells (Fig. 1H, upper row; Fig. S1E,H, left panels), THP-1 monocytes (Fig. 1H, middle row; Fig. S1E,H, right panels) and blood-derived neutrophils (Fig. 1H, lower row) to activated endothelium. Together, these results demonstrate that LT $\beta$ R ligation activates both the canonical and non-canonical NF- $\kappa$ B signaling pathways and drives inflammatory activation of ECs.

### Inflammatory activation of ECs in response to LT $\beta$ R ligation is NIK dependent

To determine whether LT $\beta$ R-induced canonical NF- $\kappa$ B signaling and inflammatory activation of ECs is NIK dependent, we transfected ECs with either scrambled small interfering RNA (siRNA; siScr) or siRNA targeting NIK (siNIK) (Fig. S3), and stimulated them with LT $\beta$  or LIGHT for short (up to 30 min) or long (3 h) time points. Knockdown of NIK in ECs had no effect on the acute activation of canonical NF- $\kappa$ B upon LT $\beta$ R ligation (Fig. S4A,B), whereas after 3 h of stimulation with LT $\beta$  or LIGHT, both HUVECs (Fig. 2A; Fig. S5A) and EA.hy926 cells (Fig. S5E) transfected with siRNA targeting NIK exhibited significantly impaired activation of canonical NF- $\kappa$ B signaling. Accordingly, NIK knockdown in HUVECs (Fig. 2B; Fig. S2B) and EA.hy926 cells (Figs S2C, S5F) resulted in decreased p50 nuclear translocation in response to long-term stimulation with LT $\beta$  or LIGHT compared with cells transfected with siScr.

Having demonstrated that NIK regulates canonical NF- $\kappa$ B signaling downstream of the LT $\beta$ R, we next explored whether NIK activity is required also for the inflammatory activation of ECs in response to LT $\beta$ R ligation. Knockdown of NIK impaired inflammatory activation (expression of inflammatory cytokines and adhesion molecules) of ECs in response to LT $\beta$ R ligation (Fig. 2C–E; Fig. S5B,C,H), and led to diminished adhesion of Jurkat T cells (Fig. 2F; Fig. S5D, left panel) and THP-1 monocytes (Fig. 2G; Fig. S5D, right panel) to EC monolayers. Similar effects were obtained in ECs treated with the pharmacological NIK inhibitor to block NIK kinase activity (Fig. 2H–J; Figs S4C,D, S5G and S6A,B), indicating that the capacity of LT $\beta$ R to sustain long-term phosphorylation of I $\kappa$ B $\alpha$  in ECs requires accumulation and kinase activity of NIK.

As complement to the loss-of-function experiments, we next overexpressed NIK in ECs. HUVECs were infected with adenoviral vectors expressing wild-type NIK (AdNIK-WT), kinase-dead NIK (AdNIK-KD) or GFP (AdGFP) as a control. NIK overexpression in HUVECs induced ligand-independent activation of the canonical NF- $\kappa$ B pathway in a concentration-dependent manner [increased levels of phospho-I $\kappa$ B $\alpha$  (p-I $\kappa$ B $\alpha$ ) and p50/p65 nuclear

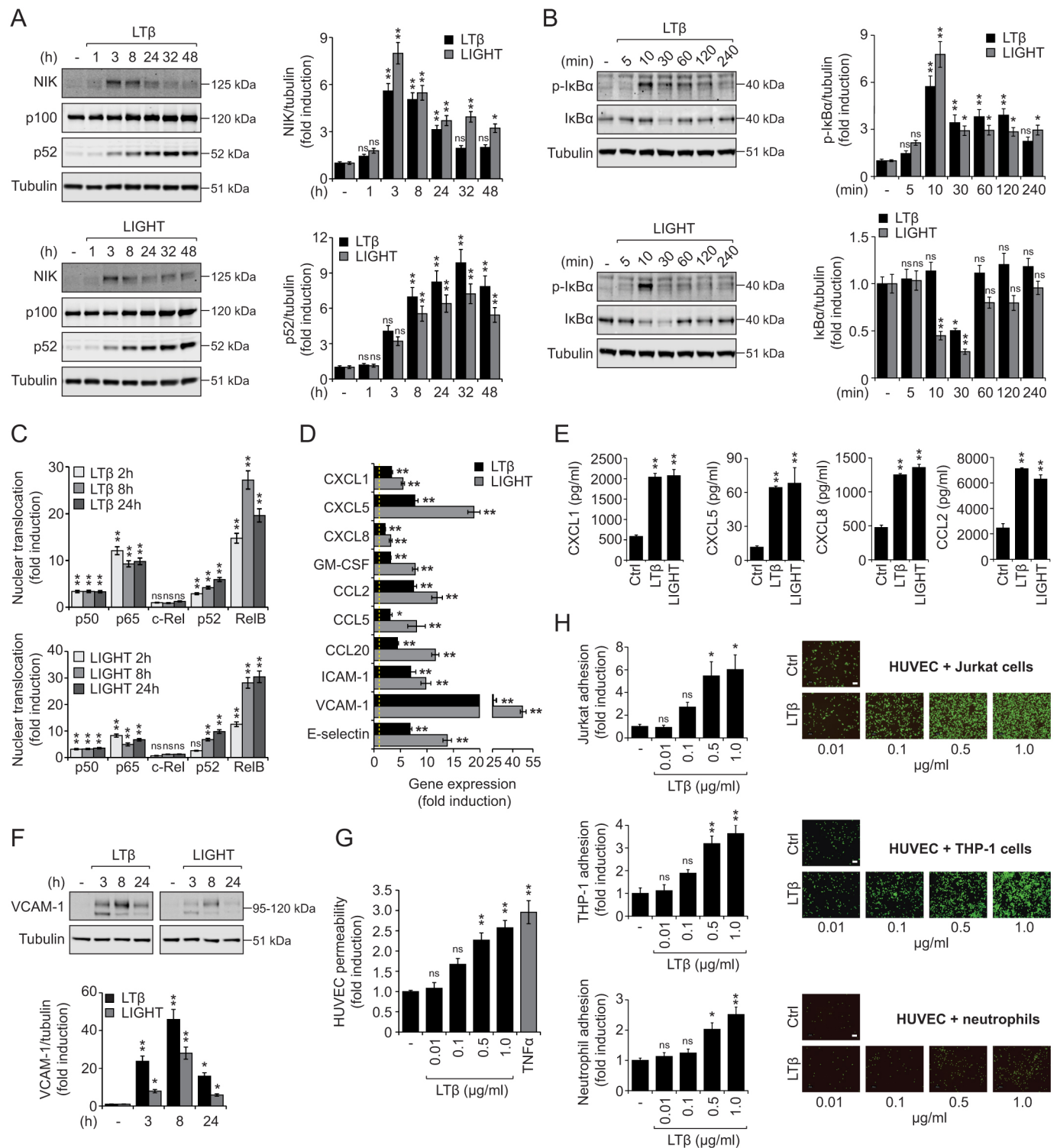


Fig. 1. See next page for legend.

translocation], whereas transduction with AdGFP or AdNIK-KD vectors did not (Fig. 3A,B; Fig. S2D), confirming the conclusion based on pharmacological inhibition of NIK that NIK kinase activity is required for the activation of the canonical NF- $\kappa$ B pathway in ECs. In line with these results, overexpression of wild-type NIK in HUVECs resulted in increased expression of inflammatory cytokines and adhesion molecules compared with cells transduced with AdGFP or AdNIK-KD (Fig. 3C,D). Together,

these data show that accumulation of kinase active NIK is required for full activation of the canonical NF- $\kappa$ B pathway and inflammatory activation of ECs in response to LT $\beta$ R ligation.

#### Dispensable role of p100 in NIK-dependent activation of canonical NF- $\kappa$ B signaling in response to LT $\beta$ R ligation

NIK activates the non-canonical NF- $\kappa$ B pathway by inducing phosphorylation of IKK $\alpha$  and p100, leading to p100 processing to

### Fig. 1. LT $\beta$ R ligation induces canonical and non-canonical NF- $\kappa$ B signaling and drives inflammatory activation of ECs.

(A) Immunoblot analysis of NIK, p100/p52 and tubulin as a loading control in HUVECs treated with LT $\beta$  (0.1  $\mu$ g/ml) or LIGHT (0.1  $\mu$ g/ml) for the indicated time points. Left panels: immunoblotting data from representative experiments. h, hours. Right panels: densitometric analysis of NIK and p52 bands from three independent experiments. (B) Immunoblot analysis of phospho-I $\kappa$ B $\alpha$  (p-I $\kappa$ B $\alpha$ ; Ser32/36), I $\kappa$ B $\alpha$  and tubulin as a loading control in HUVECs treated with LT $\beta$  (0.1  $\mu$ g/ml) or LIGHT (0.1  $\mu$ g/ml) for the indicated time points. Left panels: immunoblotting data from representative experiments. min, minutes. Right panels: densitometric analysis of p-I $\kappa$ B $\alpha$  and I $\kappa$ B $\alpha$  bands from three independent experiments. (C) Quantification of NF- $\kappa$ B DNA binding activity by ELISA in nuclear protein extracts from HUVECs treated with LT $\beta$  (0.25  $\mu$ g/ml) or LIGHT (0.25  $\mu$ g/ml) for the indicated time points. (D) Real-time qPCR quantification of the *CXCL1*, *CXCL5*, *CXCL8*, *GM-CSF*, *CCL2*, *CCL5*, *CCL20*, *ICAM-1*, *VCAM-1* and E-selectin transcripts expressed in HUVECs treated with LT $\beta$  (0.25  $\mu$ g/ml) or LIGHT (0.25  $\mu$ g/ml) for 6 h. (E) Quantification of CXCL1, CXCL5, CXCL8 and CCL2 protein levels by MSD immunoassay platform in conditioned medium from HUVECs treated with LT $\beta$  (0.25  $\mu$ g/ml) or LIGHT (0.25  $\mu$ g/ml) for 24 h. (F) Immunoblot analysis of VCAM-1 and tubulin as a loading control in HUVECs treated with LT $\beta$  (0.25  $\mu$ g/ml) or LIGHT (0.25  $\mu$ g/ml) for the indicated time points. Upper panel: immunoblotting data from a representative experiment. h, hours. Lower panel: densitometric analysis of VCAM-1 bands from three independent experiments. (G) Quantification of permeability of HUVEC monolayers treated with the indicated concentrations of LT $\beta$  or TNF $\alpha$  (0.01  $\mu$ g/ml) for 24 h. (H) Adhesion of Jurkat cells (upper row), THP-1 cells (middle row) or human blood-derived neutrophils (lower row) to HUVECs treated with the indicated concentrations of LT $\beta$  for 24 h. Left panels: quantification of immune cell adhesion to HUVECs relative to control cells. Right panels: representative images of calcein-labeled leukocytes attached to HUVECs. Scale bars: 100  $\mu$ m. Data represent mean  $\pm$  s.e.m. of three (A–D, F–H) or four (E) independent experiments. ns, not significant; \* $P$   $\leq$  0.05, \*\* $P$   $\leq$  0.01 versus control (one-way ANOVA and Tukey's HSD post hoc test).

p52 protein and its nuclear translocation (Ling et al., 1998; Xiao et al., 2001). To explore whether NIK-dependent regulation of canonical NF- $\kappa$ B signaling in ECs is mediated by p100, we knocked down p100 expression using an siRNA approach before stimulation with LT $\beta$  or LIGHT. Silencing p100 expression in HUVECs and EA.hy926 cells had no effect on LT $\beta$ R-induced activation of canonical NF- $\kappa$ B signaling (Fig. 4A,B) and did not affect the inflammatory activation of ECs in response to LT $\beta$ R ligation, as shown by unaffected gene expression of inflammatory molecules (Fig. 4C) and immune cell adhesion to activated endothelium (Fig. 4D). To specifically show that NIK-mediated regulation of canonical NF- $\kappa$ B activity in response to LT $\beta$ R ligation is p100 independent, p100 expression in HUVECs was knocked down using siRNA before overexpression of wild-type NIK (AdNIK-WT) or the control vector (AdGFP). Enhanced activation of the canonical NF- $\kappa$ B pathway induced by NIK overexpression in ECs was not impaired by p100 knockdown (Fig. 4E), suggesting that NIK-mediated activation of the canonical NF- $\kappa$ B pathway downstream of the LT $\beta$ R is direct and independent of activation of non-canonical NF- $\kappa$ B signaling.

### NIK drives inflammatory activation of ECs upon LT $\beta$ R ligation through the IKK complex

To explore whether NIK and the IKK complex interact to regulate LT $\beta$ R-induced inflammatory activation of ECs by driving sustained phosphorylation of I $\kappa$ B $\alpha$ , we silenced IKK $\alpha$  in ECs before stimulation with LT $\beta$  or LIGHT. In both HUVECs (Fig. 5A) and EA.hy926 cells (Fig. S7A), IKK $\alpha$  knockdown resulted in significantly decreased activation of canonical NF- $\kappa$ B signaling in response to stimulation with LT $\beta$  or LIGHT. Also, IKK $\alpha$  knockdown resulted in impaired inflammatory activation in response to LT $\beta$ R ligation, as shown by significantly decreased gene expression of

inflammatory cytokines and adhesion molecules compared with siScr cells (Fig. 5B). Furthermore, siRNA-mediated knockdown of IKK $\alpha$  in HUVECs that overexpressed NIK (AdNIK-WT) effectively blocked activation of the canonical NF- $\kappa$ B pathway (Fig. 5C) and inflammatory activation (gene expression of inflammatory cytokines and adhesion molecules) (Fig. 5D). Therefore, IKK $\alpha$  activity appears essential for NIK-dependent activation of canonical NF- $\kappa$ B signaling pathway downstream of LT $\beta$ R ligation.

IKK $\alpha$  and IKK $\beta$  both phosphorylate the I $\kappa$ B proteins, leading to the subsequent activation of NF- $\kappa$ B. However, IKK $\beta$  exhibits stronger kinase activity for the I $\kappa$ B proteins and evokes a more robust activation of the canonical NF- $\kappa$ B pathway than IKK $\alpha$  (Woronicz et al., 1997; Li et al., 1998, 1999; Hu et al., 1999; Tanaka et al., 1999; Adli et al., 2010), implicating IKK $\beta$  in the induction of the canonical NF- $\kappa$ B pathway downstream of the NIK–IKK $\alpha$  axis in ECs in response to LT $\beta$ R ligation. In support of this hypothesis, activation of IKK $\alpha$  in response to either TNF $\alpha$  or overexpression of NIK has been shown to result in phosphorylation and activation of IKK $\beta$  (O'Mahony et al., 2000; Yamamoto et al., 2000). To determine the role of IKK $\beta$  in mediating the pro-inflammatory activity of the NIK–IKK $\alpha$  axis in ECs upon LT $\beta$ R ligation, the effect of pharmacological inhibition of IKK $\beta$  kinase activity or siRNA-mediated knockdown of IKK $\beta$  on LT $\beta$ R-induced I $\kappa$ B $\alpha$  phosphorylation was studied. Both HUVECs and EA.hy926 cells treated with an IKK $\beta$  inhibitor (IKK $\beta$ i) exhibited complete inhibition of canonical NF- $\kappa$ B signaling (Fig. 6A; Figs S6C,D and S7B), and, in HUVECs, a strong reduction in inflammatory activation (decreased expression of inflammatory cytokines and adhesion molecules as well as diminished adhesion of immune cells) in response to LT $\beta$ R ligation was observed (Fig. 6B–E). Similarly, siRNA-mediated knockdown of IKK $\beta$  in HUVECs resulted in inhibition of canonical NF- $\kappa$ B signaling (Fig. S7C,D), and a strong reduction in inflammatory activation (decreased expression of inflammatory cytokines and adhesion molecules) in response to LT $\beta$ R ligation (Fig. S7E).

To unambiguously show that IKK $\beta$  acts downstream of the NIK–IKK $\alpha$  axis in activating canonical NF- $\kappa$ B signaling, HUVECs overexpressing NIK (AdNIK-WT) were treated with the IKK $\beta$ i or dimethyl sulfoxide (DMSO) as a control, followed by analysis of p-I $\kappa$ B $\alpha$  and gene expression. IKK $\beta$  inhibition resulted in profound suppression of NIK-mediated activation of canonical NF- $\kappa$ B signaling, placing NIK upstream of IKK $\beta$  in activating the canonical NF- $\kappa$ B pathway in response to LT $\beta$ R ligation (Fig. 6F). In line with these data, inhibition of IKK $\beta$  in HUVECs overexpressing NIK resulted in decreased inflammatory activation of these cells (Fig. 6G). Taken together, our data demonstrate that NIK regulates the canonical NF- $\kappa$ B signaling pathway downstream of LT $\beta$ R ligation by amplifying IKK complex activity.

### NIK is involved in inflammatory activation of ECs induced by RA synovial fluid

Synovial fluid obtained from RA patients contains high levels of pro-inflammatory stimuli, including LT $\beta$ , LIGHT, CD40 and BAFF (also known as TNFSF13B), which are all able to induce NIK and non-canonical NF- $\kappa$ B signaling downstream of their respective receptors (Noort et al., 2015b; Maracle et al., 2017). Moreover, NIK is highly expressed in blood vessels in RA synovial tissues (Noort et al., 2014; Noort et al., 2015a), suggesting a role for NIK in inflammatory activation of ECs in RA. To explore whether NIK-mediated inflammatory activation of the endothelium might be a relevant biological driver of disease, HUVECs were stimulated with four different pools of RA synovial fluid (RASf) and then analyzed

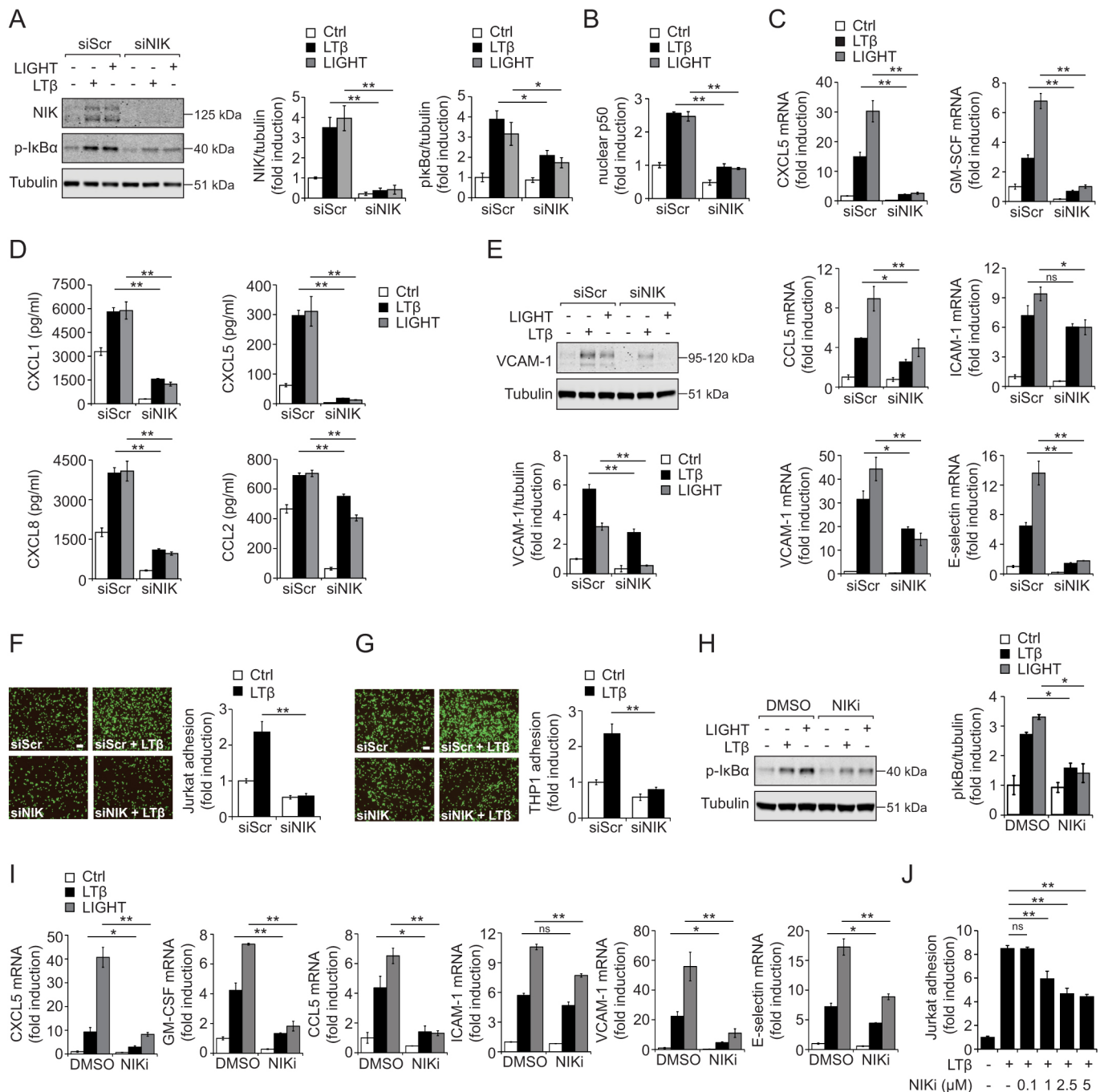


Fig. 2. See next page for legend.

for the induction of NF- $\kappa$ B signaling and inflammatory activation. RASF activated both the non-canonical and canonical NF- $\kappa$ B pathways in a concentration-dependent manner in HUVECs, as shown by increased levels of p52 and p-I $\kappa$ B $\alpha$ , respectively (Fig. 7A). In addition, RASF-treated HUVECs exhibited increased expression of inflammatory cytokines and adhesion molecules, indicating inflammatory activation of ECs in response to RASF treatment (Fig. 7B). Knockdown of NIK, as shown by impaired generation of p52, resulted in reduced activation of canonical NF- $\kappa$ B signaling induced by RASF treatment (Fig. 7C). This effect translated to diminished inflammatory activation of ECs, as shown by decreased gene expression of inflammatory cytokines and adhesion molecules after RASF treatment (Fig. 7D),

suggesting that NIK is important for inflammatory activation of ECs in RA (Fig. 8).

## DISCUSSION

Here, we provide evidence that LT $\beta$ R signaling drives inflammatory activation of endothelium through the canonical NF- $\kappa$ B pathway in a manner dependent on accumulation of NIK protein. Furthermore, we show that NIK activates the canonical NF- $\kappa$ B pathway by enhancing IKK complex activity, implicating NIK as a proximal signaling molecule that activates both the canonical and non-canonical NF- $\kappa$ B pathways downstream of LT $\beta$ R. The observation that LT $\beta$ R stimulation can drive inflammatory activation of ECs through NF- $\kappa$ B is in line with a previous report (Madge et al., 2008),

**Fig. 2. NIK is required for the induction of canonical NF- $\kappa$ B pathway and inflammatory activation of ECs upon LT $\beta$ R ligation.** (A) Immunoblot analysis of NIK, p-I $\kappa$ B $\alpha$  (Ser32/36) and tubulin as a loading control in HUVECs transfected with scrambled siRNA (siScr; 10 nM) or siRNA targeting NIK (siNIK; 10 nM) and stimulated with LT $\beta$  (0.25  $\mu$ g/ml) or LIGHT (0.25  $\mu$ g/ml) for 3 h. Cells were incubated with the proteasome inhibitor MG132 (50  $\mu$ M) for the final hour to prevent NIK and p-I $\kappa$ B $\alpha$  degradation. Left panel: immunoblotting data from a representative experiment. Middle and right panels: densitometric analysis of NIK and p-I $\kappa$ B $\alpha$  bands from seven independent experiments. (B) Quantification of p50 DNA-binding activity by ELISA in nuclear protein extracts from HUVECs transfected with siScr or siNIK as in A, and stimulated with LT $\beta$  (0.25  $\mu$ g/ml) or LIGHT (0.25  $\mu$ g/ml) for 6 h. (C) Real-time qPCR quantification of the *CXCL5*, *GM-CSF*, *CCL5*, *ICAM-1*, *VCAM-1* and E-selectin transcripts expressed in HUVECs transfected with siScr or siNIK as in A, and stimulated with LT $\beta$  (0.25  $\mu$ g/ml) or LIGHT (0.25  $\mu$ g/ml) for 6 h. (D) Quantification of CXCL1, CXCL5, CXCL8 and CCL2 protein levels by MSD immunoassay platform in conditioned medium from HUVECs transfected with siScr or siNIK as in A, and stimulated with LT $\beta$  (0.25  $\mu$ g/ml) or LIGHT (0.25  $\mu$ g/ml) for 24 h. (E) Immunoblot analysis of VCAM-1 and tubulin as a loading control in HUVECs transfected with siScr or siNIK as in A, and stimulated with LT $\beta$  (0.25  $\mu$ g/ml) or LIGHT (0.25  $\mu$ g/ml) for 24 h. Upper panel: immunoblotting data from a representative experiment. Lower panel: densitometric analysis of VCAM-1 bands from three independent experiments. (F,G) Adhesion of Jurkat cells (F) or THP-1 cells (G) to HUVECs transfected with siScr or siNIK as in A and incubated with LT $\beta$  (0.25  $\mu$ g/ml) for 24 h. Left panels: representative images of calcein-labeled leukocytes attached to HUVECs. Scale bars: 100  $\mu$ m. Right panels: quantification of immune cell adhesion to HUVECs relative to siScr. (H) Immunoblot analysis of p-I $\kappa$ B $\alpha$  (Ser32/36) and tubulin as a loading control in HUVECs treated with DMSO or NIK inhibitor (NIKI; 2.5  $\mu$ M) for 30 min, followed by stimulation with LT $\beta$  (0.25  $\mu$ g/ml) or LIGHT (0.25  $\mu$ g/ml) for 3 h. Cells were treated with proteasome inhibitor MG132 (50  $\mu$ M) for the final hour to prevent p-I $\kappa$ B $\alpha$  degradation. Left panel: immunoblotting data from a representative experiment. Right panel: densitometric analysis of p-I $\kappa$ B $\alpha$  bands from two independent experiments. (I) Real-time qPCR quantification of the *CXCL5*, *GM-CSF*, *CCL5*, *ICAM-1*, *VCAM-1* and E-selectin transcripts expressed in HUVECs treated with DMSO or NIKi as in H, followed by stimulation with LT $\beta$  (0.25  $\mu$ g/ml) or LIGHT (0.25  $\mu$ g/ml) for 6 h. (J) Adhesion of Jurkat cells to HUVECs treated with DMSO or the indicated concentrations of NIKi for 30 min, followed by stimulation with LT $\beta$  (0.25  $\mu$ g/ml) for 24 h. Data represent mean $\pm$ s.e.m. of two (H), three (B,C,E–G,I,J), four (D) or seven (A) independent experiments. ns, not significant; \* $P$  $\leq$ 0.05, \*\* $P$  $\leq$ 0.01 [one-way ANOVA and Tukey's HSD post hoc test (A–E,H–J) or Student's  $t$ -test (F,G)].

except that, in this study, the authors did not identify NIK as a regulator of the canonical NF- $\kappa$ B pathway, as they focused on immediate events after receptor ligation rather than sustained signaling through NIK. Our study clearly shows that accumulation of kinase active NIK over time is required for full activation of the canonical NF- $\kappa$ B pathway and inflammation in ECs in response to LT $\beta$ R ligation, distinguishing it from NF- $\kappa$ B signaling induced by e.g. TNF $\alpha$  and IL-1 $\beta$ .

As was previously demonstrated in other cell types (Matsushima et al., 2001; Smith et al., 2001; Yin et al., 2001; Ramakrishnan et al., 2004; Zarnegar et al., 2008), we found that NIK is required for phosphorylation of I $\kappa$ B $\alpha$  in ECs, indicating that NIK regulates NF- $\kappa$ B signaling through activation of the IKK complex downstream of the LT $\beta$ R in ECs. We also show that p100 is dispensable for NIK-dependent activation of the IKK complex and phosphorylation of I $\kappa$ B $\alpha$  upon LT $\beta$ R ligation. Interestingly, it has been previously reported that the canonical NF- $\kappa$ B pathway can be regulated independently of the IKK complex through the C-terminus of p100 (termed I $\kappa$ B $\delta$ ; also known as NFKBID), which, acting as an I $\kappa$ B protein, can bind canonical Rel proteins and thereby prevent their nuclear translocation (Scheinman et al., 1993; Novack et al., 2003). This suggests that NIK-dependent activation of canonical NF- $\kappa$ B activity upon LT $\beta$ R ligation could result from a combination of increased induction of the IKK complex and processing of the C-terminus of p100. However, we observed that inflammatory

activation of ECs in response to LT $\beta$ R ligation is p100 independent, indicating that p100-mediated activation of canonical NF- $\kappa$ B signaling may be cell-type or stimulus specific, which remains to be determined in future studies.

Moreover, we demonstrate that IKK $\alpha$  and IKK $\beta$  are required for NIK-dependent activation of the canonical NF- $\kappa$ B pathway downstream of the LT $\beta$ R in ECs, although the reciprocal regulation of IKK $\alpha$  and IKK $\beta$  is not distinguished. However, based on previous reports showing that activation of IKK $\alpha$  by NIK leads to phosphorylation and activation of IKK $\beta$ , and subsequently to IKK $\beta$ -mediated phosphorylation of I $\kappa$ B $\alpha$  (Woronicz et al., 1997), it is likely that this mechanism also accounts for canonical NF- $\kappa$ B activation in ECs upon LT $\beta$ R ligation or NIK overexpression. Whether stimulation of other TNFR superfamily members, like CD40, also results in NIK-mediated activation of canonical NF- $\kappa$ B signaling in ECs remains to be determined (Seigner et al., 2018).

We show that NIK and IKK $\alpha$  are required for sustained activation of the canonical NF- $\kappa$ B pathway through the IKK complex in response to LT $\beta$ R ligation in ECs, but we cannot exclude that other mechanisms mediated by these kinases may regulate the canonical NF- $\kappa$ B pathway and inflammatory activation of endothelium downstream of LT $\beta$ R ligation. For instance, IKK $\alpha$  has also been described to have nuclear functions and serve as a regulator of canonical NF- $\kappa$ B dependent gene expression through control of promoter-associated, cytokine-induced phosphorylation and subsequent acetylation of specific residues in histone H3 (Anest et al., 2003; Yamamoto et al., 2003). In this context, NIK may regulate phosphorylation of histone H3 by inducing phosphorylation and activation of IKK $\alpha$  (Park et al., 2006). Alternatively, LT $\beta$ R ligation may induce NIK-mediated activation of STAT3 as observed in prostate cancer cells (Nadiminty et al., 2007). STAT3 has been shown to maintain constitutive NF- $\kappa$ B activity and act synergistically with NF- $\kappa$ B to regulate several pro-inflammatory genes (e.g. IL-6) (Lee et al., 2009; Yoon et al., 2012; Yu et al., 2014), and it is possible that STAT3 is involved in NIK-dependent inflammatory activation of ECs in response to LT $\beta$ R.

In regards to the relevance for chronic inflammatory diseases, we demonstrate that treatment of ECs with RASF drives activation of both canonical and non-canonical NF- $\kappa$ B signaling and inflammatory activation of ECs. This is in agreement with previous reports showing that stimuli that are able to induce canonical and non-canonical NF- $\kappa$ B signaling are abundantly present in the inflamed joints of RA patients, i.e. in synovial tissue or fluid, along with expression of the corresponding receptors on the surface of ECs (Noort et al., 2015b; Maracle et al., 2017). Consequently, both canonical and non-canonical NF- $\kappa$ B pathways are activated in blood vessels of the inflamed RA synovium (Noort et al., 2014, 2015a; Maracle et al., 2017). Importantly, our data further show that inhibition of NIK activity in ECs impairs activation of the canonical NF- $\kappa$ B pathway and prevents the induction of a pro-inflammatory phenotype in response to RASF, implicating NIK as a key regulator of pathological, inflammatory activation of endothelium. The incomplete inhibition of RASF-induced inflammatory activation of ECs after targeting NIK is likely explained by the composition of RASF, which is known to contain a plethora of pro-inflammatory molecules, including TNF $\alpha$  and IL-1 $\beta$ , which are capable of inducing canonical NF- $\kappa$ B signaling and inflammatory responses in ECs independently of NIK (Matsushima et al., 2001; Yin et al., 2001; Ramakrishnan et al., 2004).

In preclinical models, it has been established that mice lacking NIK are resistant to arthritis induction in the adjuvant-induced arthritis model, and have reduced inflammation-induced angiogenesis, osteoclastogenesis and bone erosions (Aya et al.,

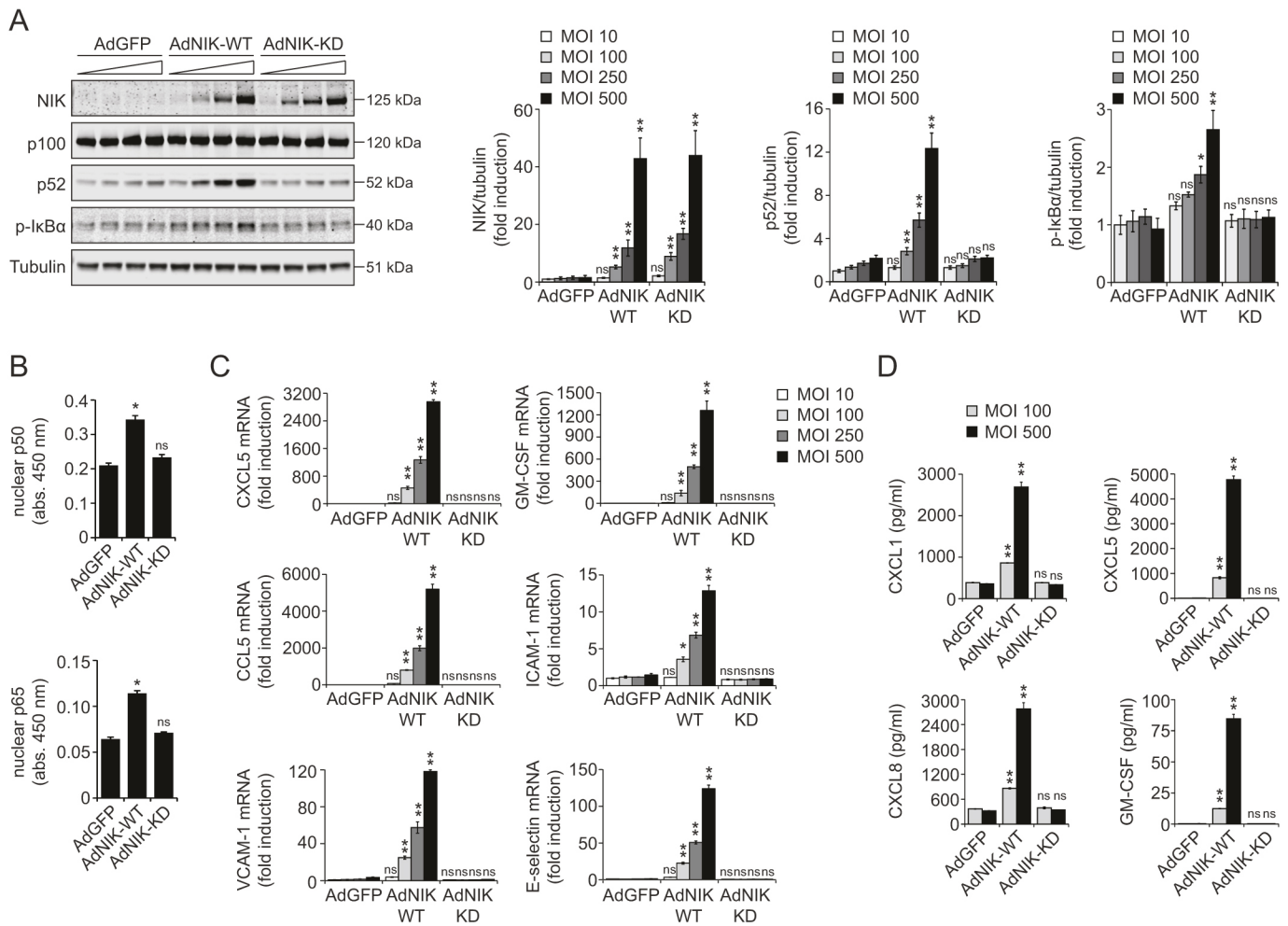


**Fig. 3. Ligand-independent activation of canonical NF- $\kappa$ B pathway in ECs overexpressing NIK.** (A) Immunoblot analysis of NIK, p100/p52, p-I $\kappa$ B $\alpha$  (Ser32/36) and tubulin as a loading control in HUVECs transduced with adenoviral vectors expressing GFP (AdGFP), wild-type NIK (AdNIK-WT) or kinase-dead NIK (AdNIK-KD) at 10, 100, 250 and 500 multiplicities of infection (MOIs). Cells were treated with the proteasome inhibitor MG132 (50  $\mu$ M) for the final hour to prevent p-I $\kappa$ B $\alpha$  degradation. Left panel: immunoblotting data from a representative experiment. Right three panels: densitometric analysis of NIK, p52 and p-I $\kappa$ B $\alpha$  bands from three independent experiments. (B) Quantification of p50 and p65 DNA-binding activity by ELISA in nuclear protein extracts from HUVECs transduced with AdGFP, AdNIK-WT or AdNIK-KD (250 MOIs). (C) Real-time qPCR quantification of the *CXCL5*, *GM-CSF*, *CCL5*, *ICAM-1*, *VCAM-1* and *E-selectin* transcripts expressed in HUVECs transduced with AdGFP, AdNIK-WT or AdNIK-KD as in A. (D) Quantification of CXCL1, CXCL5, CXCL8 and GM-CSF protein levels by MSD immunoassay platform in conditioned medium from HUVECs transduced with AdGFP, AdNIK-WT or AdNIK-KD (100 and 500 MOIs). Data represent mean  $\pm$  s.e.m. of three independent experiments. ns, not significant; \* $P$   $\leq$  0.05, \*\* $P$   $\leq$  0.01 versus AdGFP (one-way ANOVA and Tukey's HSD post hoc test).

2005; Noort et al., 2014). Our finding that NIK inhibition impairs inflammatory activation of ECs in response to RASF suggests that the decreased severity of arthritis and histological inflammation scores in *Nik*<sup>-/-</sup> mice may be, at least in part, due to impaired inflammatory activation of endothelium and as a consequence of reduced influx of immune cells into the synovial tissue.

In conclusion, we demonstrate that NIK is critically involved in inflammatory activation of ECs in response to LT $\beta$ R ligation (Fig. 8), and further identify NIK as a potentially novel therapeutic target for alleviating the pathological endothelium phenotype induced by canonical and non-canonical NF- $\kappa$ B signaling at sites of chronic inflammation.

## MATERIALS AND METHODS

### Reagents

Recombinant human proteins LT $\beta$  and LIGHT were purchased from R&D Systems. Antibodies against NIK (#4994), p-I $\kappa$ B $\alpha$  (#9246), I $\kappa$ B $\alpha$  (#9242) and IKK $\alpha$  (#2682) were from Cell Signaling Technology. Antibodies

against VCAM-1 (ab134047), lamin B1 (ab133741) and  $\alpha$ -tubulin (ab4074) were from Abcam. Anti-p100/NF- $\kappa$ B2 antibody was purchased from EMD Millipore (#05-361). Antibody against  $\beta$ -actin (sc-47778) was purchased from Santa Cruz Biotechnology. MG132 and fluorescein isothiocyanate (FITC)-conjugated dextran (10 kDa) were purchased from Sigma-Aldrich. Calcein-AM was from Thermo Fisher Scientific. The pharmacological inhibitors of NIK and IKK $\beta$  were resynthesized by AstraZeneca (Gothenburg, Sweden), following the patented procedures (Andersson et al., 2008; Hynd et al., 2014). RASF was collected during mini-arthroscopy as described previously (Kraan et al., 2002), pooled from four patients and used at various concentrations. Patient consent was obtained for all participants in written format according to the Declaration of Helsinki.

### Cell culture

Primary HUVECs were obtained from Lonza and cultured in MCDB131 medium (Gibco) supplemented with 2 mM L-glutamine (Gibco) and Low Serum Growth Supplement (Gibco), containing 2% v/v fetal bovine serum (FBS), 1  $\mu$ g/ml hydrocortisone, 10 ng/ml human epidermal growth factor, 3 ng/ml basic fibroblast growth factor and 10  $\mu$ g/ml heparin. HUVECs were passaged using trypsin/EDTA (0.05%; Gibco), and all experiments were

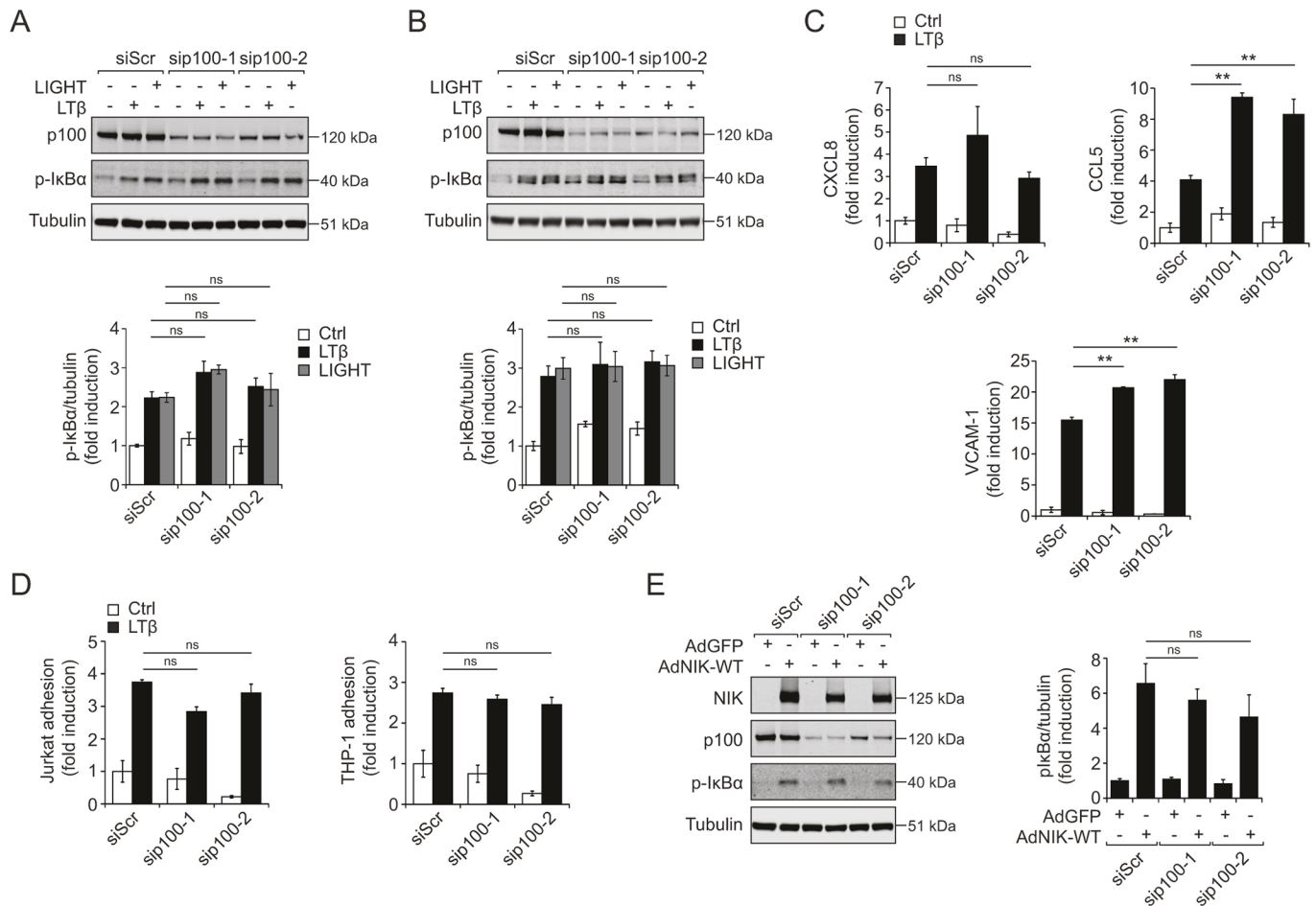


**Fig. 4. Dispensable role of p100 in NIK-driven activation of canonical NF- $\kappa$ B pathway in ECs upon LT $\beta$ R ligation.** (A,B) Immunoblot analysis of p100, p-I $\kappa$ B $\alpha$  (Ser32/36) and tubulin as a loading control in HUVECs (A) and EA.hy926 cells (B) transfected with scrambled siRNA (siScr; 10 nM) or siRNAs targeting p100 (sip100-1 or sip100-2; 10 nM) and stimulated with LT $\beta$  (0.25  $\mu$ g/ml) or LIGHT (0.25  $\mu$ g/ml) for 3 h. Cells were incubated with the proteasome inhibitor MG132 (50  $\mu$ M) for the final hour to prevent p-I $\kappa$ B $\alpha$  degradation. Upper panels: immunoblotting data from representative experiments. Lower panels: densitometric analysis of p-I $\kappa$ B $\alpha$  bands from three independent experiments. (C) Real-time qPCR quantification of the *CXCL8*, *CCL5* and *VCAM-1* transcripts expressed in HUVECs transfected with siScr or sip100 as in A and stimulated with LT $\beta$  (0.25  $\mu$ g/ml) for 6 h. (D) Adhesion of Jurkat cells (left panel) and THP-1 cells (right panel) to HUVECs transfected with siScr or sip100 as in A, and stimulated with LT $\beta$  (0.25  $\mu$ g/ml) for 24 h. (E) Immunoblot analysis of NIK, p100, p-I $\kappa$ B $\alpha$  (Ser32/36) and tubulin as a loading control in HUVECs transfected with siScr or sip100 as in A, and transduced with adenoviral vectors expressing GFP (AdGFP) or wild-type NIK (AdNIK-WT) at 250 MOIs. Cells were incubated with the proteasome inhibitor MG132 (50  $\mu$ M) for the final hour to prevent p-I $\kappa$ B $\alpha$  degradation. Left panel: immunoblotting data from a representative experiment. Right panel: densitometric analysis of p-I $\kappa$ B $\alpha$  bands from three independent experiments. Data represent mean  $\pm$  s.e.m. of two (C), three (A,B,E) or four (D) independent experiments. ns, not significant; \*\* $P$   $\leq$  0.01 (one-way ANOVA and Tukey's HSD post hoc test).

performed using cells at passage 2–5. Primary HMVECs were purchased from American Type Culture Collection (ATCC) and cultured in Vascular Cell Basal Medium (ATCC) supplemented with the Microvascular Endothelial Cell Growth Kit-VEGF (ATCC). EA.hy926 cells were obtained from ATCC and cultured in Dulbecco's modified Eagle Medium (DMEM) (Gibco) supplemented with 10% v/v FBS, 2 mM L-glutamine, 100 U/ml penicillin and 100  $\mu$ g/ml streptomycin (Gibco). Jurkat and THP-1 cells were obtained from ATCC and cultured in RPMI-1640 medium (Gibco) supplemented with 10% v/v FBS, 2 mM L-glutamine, 100 U/ml penicillin and 100  $\mu$ g/ml streptomycin. Human neutrophils were isolated from freshly drawn anti-coagulated whole blood using a human MACSxpress<sup>TM</sup> Neutrophil Isolation Kit (Miltenyi Biotec), according to the manufacturer's recommendations. Isolated neutrophils were kept in serum-free RPMI-1640 medium and used in the experiments shortly after isolation. Cell culture was performed in a humidified incubator maintained at 37°C with 5% CO<sub>2</sub> and 95% air. Cells were routinely tested for mycoplasma contamination.

#### Western blot analysis

Cells were lysed in ice-cold radioimmunoprecipitation assay (RIPA) buffer (10 mM Tris-HCl at pH 7.4, 150 mM NaCl, 1 mM EDTA, 0.1% SDS, 1%

Triton X-100 and 1% sodium deoxycholate) supplemented with protease inhibitors (Complete Protease Inhibitor Mixture Tablets, Roche) and phosphatase inhibitors (Phosphatase Inhibitor Cocktail Tablets, Roche). Protein concentration was measured with a Pierce<sup>TM</sup> BCA Protein Assay Kit (Thermo Fisher Scientific), and equal amounts of proteins were separated by SDS-PAGE. Resolved proteins were transferred to a nitrocellulose membrane, which was then blocked with 5% skim milk. After blocking, membrane was probed with primary antibodies. Proteins were visualized with IRDye secondary antibodies and Odyssey Infrared Imaging System (LI-COR Biosciences UK) or horseradish peroxidase (HRP)-conjugated secondary antibodies (Dako), LUMI-LIGHT<sup>PLUS</sup> WB Substrate (Roche) and the ImageQuant LAS 4000 imaging system (GE Healthcare). Intensities of immunoreactive bands were quantified by densitometry using Image Studio Ver. 4.0 software (LI-COR Biosciences UK).

#### NF- $\kappa$ B ELISA

Nuclear cell fractions were isolated using a Nuclear Extract Kit (Active Motif), and 2  $\mu$ g nuclear extracts was used to quantify the activation of NF- $\kappa$ B transcription factors with the enzyme-linked immunosorbent assay (ELISA)-based TransAM NF- $\kappa$ B Family Transcription Factor Assay Kit



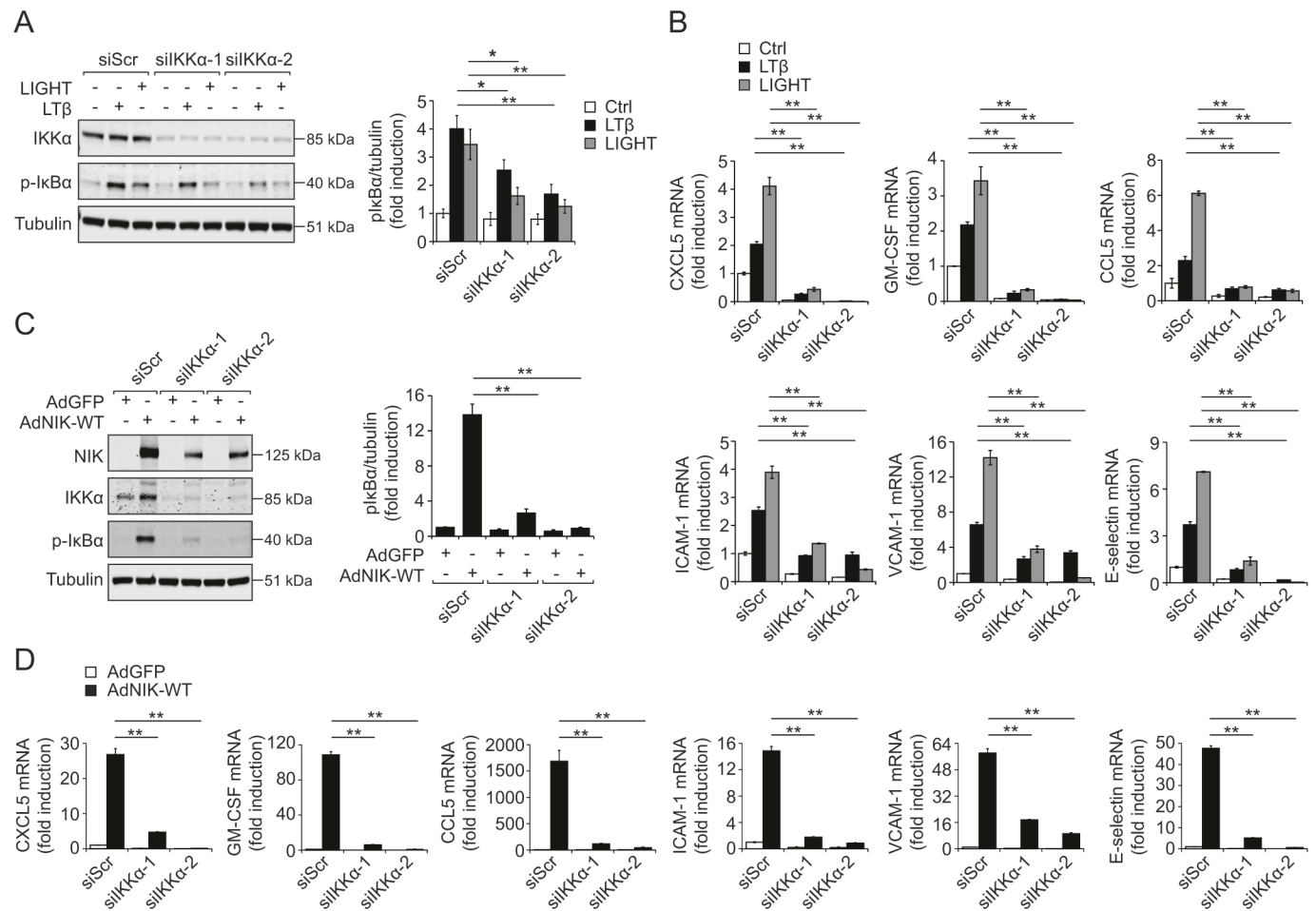


**Fig. 5. NIK-driven canonical NF- $\kappa$ B signaling in response to LT $\beta$ R ligation depends on intact IKK $\alpha$  activity.** (A) Immunoblot analysis of IKK $\alpha$ , p-I $\kappa$ B $\alpha$  (Ser32/36) and tubulin as a loading control in HUVECs transfected with scrambled siRNA (siScr; 10 nM) or siRNAs targeting IKK $\alpha$  (siIKK $\alpha$ -1 or siIKK $\alpha$ -2; 10 nM) and stimulated with LT $\beta$  (0.25  $\mu$ g/ml) or LIGHT (0.25  $\mu$ g/ml) for 3 h. Cells were incubated with the proteasome inhibitor MG132 (50  $\mu$ M) for the final hour to prevent p-I $\kappa$ B $\alpha$  degradation. Left panel: immunoblotting data from a representative experiment. Right panel: densitometric analysis of p-I $\kappa$ B $\alpha$  bands from five independent experiments. (B) Real-time qPCR quantification of the *CXCL5*, *GM-CSF*, *CCL5*, *ICAM-1*, *VCAM-1* and E-selectin transcripts expressed in HUVECs transfected with siScr or siIKK $\alpha$  as in A, and stimulated with LT $\beta$  (0.25  $\mu$ g/ml) or LIGHT (0.25  $\mu$ g/ml) for 6 h. (C) Immunoblot analysis of NIK, IKK $\alpha$ , p-I $\kappa$ B $\alpha$  (Ser32/36) and tubulin as a loading control in HUVECs transfected with siScr or siIKK $\alpha$  as in A, and transduced with adenoviral vectors expressing GFP (AdGFP) or wild-type NIK (AdNIK-WT) at 250 MOIs. Left panel: immunoblotting data from a representative experiment. Right panel: densitometric analysis of p-I $\kappa$ B $\alpha$  bands from four independent experiments. (D) Real-time qPCR quantification of the *CXCL5*, *GM-CSF*, *CCL5*, *ICAM-1*, *VCAM-1* and E-selectin transcripts expressed in HUVECs transfected with siScr or siIKK $\alpha$  as in A, and transduced with AdGFP or AdNIK-WT (250 MOIs). Data represent mean $\pm$ s.e.m. of two (B), four (C,D) or five (A) independent experiments. \* $P$ <0.05, \*\* $P$ <0.01 (one-way ANOVA and Tukey's HSD post hoc test).

(Active Motif), following the manufacturer's instructions. Nuclear extracts were plated in duplicates.

#### Quantitative RT-PCR

RNA was isolated using the RNeasy Plus Mini Kit (Qiagen) and reverse transcribed to complementary DNA (cDNA) using the High-Capacity RNA-to-cDNA Kit (Applied Biosystems). Afterwards, 30 ng cDNA was used for quantitative PCR (qPCR) in a final volume of 10  $\mu$ l, which contained TaqMan Fast Universal PCR Master Mix (Applied Biosystems) and the specific TaqMan Gene Expression Assay for the gene studied (Applied Biosystems). The following Taqman Assays were used: *CXCL1* (id: Hs00605382\_gH), *CXCL5* (id: Hs01099660\_g1), *CXCL8* (id: Hs00174103\_m1), *GM-CSF* (id: Hs00929873\_m1), *CCL2* (id: Hs00234140\_m1), *CCL5* (id: Hs00982282\_m1), *CCL20* (id: Hs00355476\_m1), *ICAM-1* (id: Hs00164932\_m1), *VCAM-1* (id: Hs01003372\_m1) and E-selectin (id: Hs00174057\_m1). PCR amplification was performed with a QuantStudio<sup>TM</sup> 7 Flex Real-Time PCR System (Applied Biosystems). The comparative  $\Delta\Delta$ CT method was used for relative quantification of gene expression on triplicates of each reaction. EDF-1 was used as an endogenous control.

#### Multiplex cytokine assays

Cytokine levels were measured in cell culture medium using Meso Scale Discovery (MSD) ELISA according to the manufacturer's instructions. MSD plates were analyzed on the MS2400 imager (MSD). All standards and samples were measured in duplicates.

#### Membrane-based antibody array

Cytokine levels were measured in cell culture medium from control or LT $\beta$ -stimulated HMVECs with a Proteome Profiler Human XL Cytokine Array according to the protocol provided by the manufacturer. The arrays were scanned and quantified with ImageJ software (National Institutes of Health). Presented data show fold change in relative protein levels (normalized to array reference) in LT $\beta$ -stimulated HMVECs compared with control cells.

#### Adhesion assay

ECs were seeded in a black 96-well plate coated with 1% fibronectin at  $1.2 \times 10^5$  cells per well in complete MCD131 medium and grown for 2 days. Cells were then washed with PBS and stimulated for 24 h with LT $\beta$

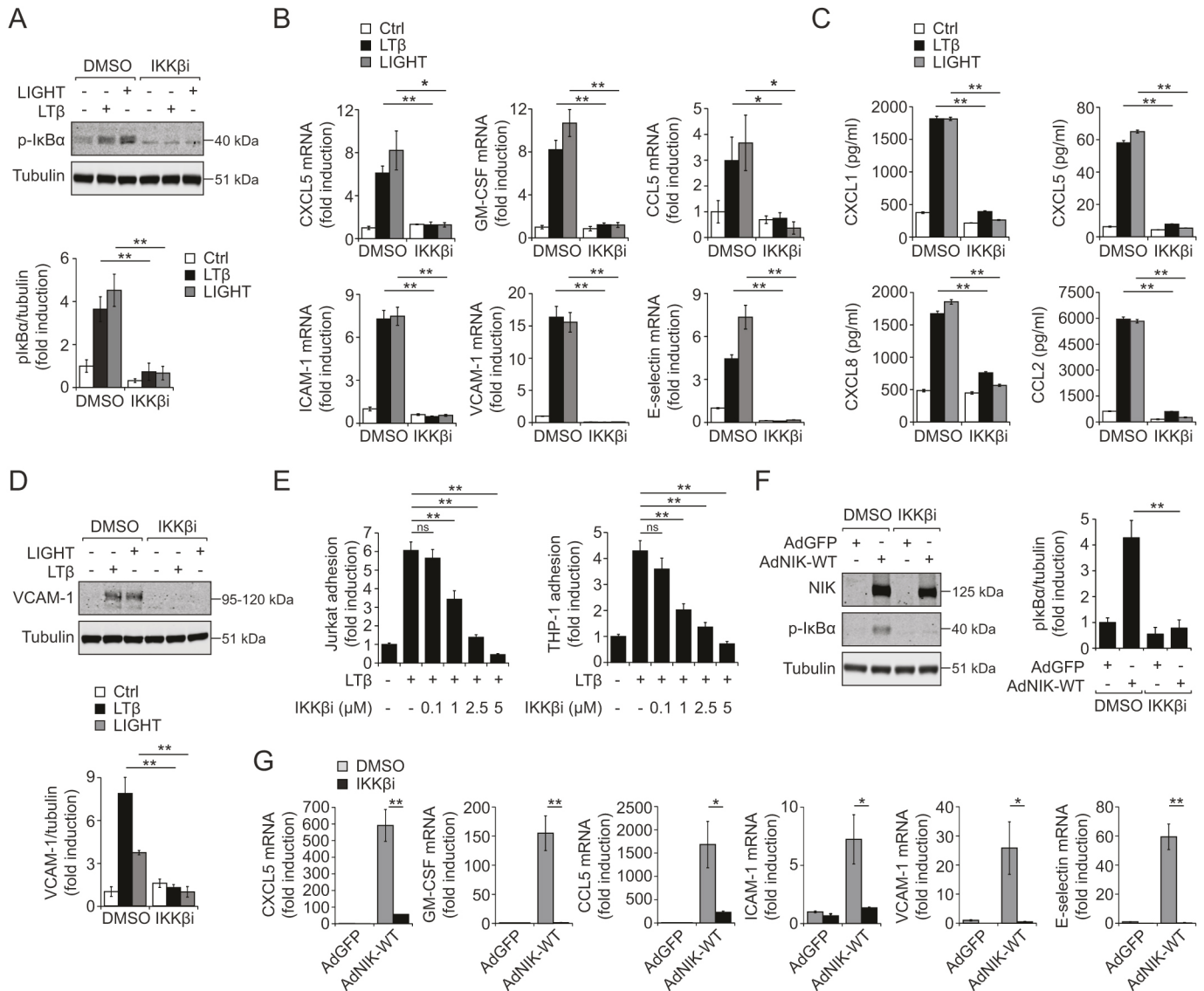


**Fig. 6. NIK-IKK $\alpha$  complex requires IKK $\beta$  for the activation of canonical NF- $\kappa$ B signaling in ECs upon LT $\beta$ R ligation.** (A) Immunoblot analysis of p-I $\kappa$ B $\alpha$  (Ser32/36) and tubulin as a loading control in HUVECs treated with DMSO or IKK $\beta$  inhibitor (IKK $\beta$ i; 2.5  $\mu$ M) for 30 min, followed by stimulation with LT $\beta$  (0.25  $\mu$ g/ml) or LIGHT (0.25  $\mu$ g/ml) for 3 h. Cells were incubated with the proteasome inhibitor MG132 (50  $\mu$ M) for the final hour to prevent p-I $\kappa$ B $\alpha$  degradation. Upper panel: immunoblotting data from a representative experiment. Lower panel: densitometric analysis of p-I $\kappa$ B $\alpha$  bands from four independent experiments. (B) Real-time qPCR quantification of the *CXCL5*, *GM-CSF*, *CCL5*, *ICAM-1*, *VCAM-1* and E-selectin transcripts expressed in HUVECs treated with DMSO or IKK $\beta$ i as in A, followed by stimulation with LT $\beta$  (0.25  $\mu$ g/ml) or LIGHT (0.25  $\mu$ g/ml) for 6 h. (C) Quantification of CXCL1, CXCL5, CXCL8 and CCL-2 protein levels by MSD immunoassay platform in conditioned medium from HUVECs treated with DMSO or IKK $\beta$ i as in A, followed by stimulation with LT $\beta$  (0.25  $\mu$ g/ml) or LIGHT (0.25  $\mu$ g/ml) for 24 h. (D) Immunoblot analysis of VCAM-1 and tubulin as a loading control in HUVECs treated with DMSO or IKK $\beta$ i as in A, followed by stimulation with LT $\beta$  (0.25  $\mu$ g/ml) or LIGHT (0.25  $\mu$ g/ml) for 24 h. Upper panel: immunoblotting data from a representative experiment. Lower panel: densitometric analysis of VCAM-1 bands from three independent experiments. (E) Adhesion of Jurkat cells (left panel) and THP-1 cells (right panel) to HUVECs treated with DMSO or IKK $\beta$ i at the indicated concentrations for 30 min, followed by stimulation with LT $\beta$  (0.25  $\mu$ g/ml) for 24 h. (F) Immunoblot analysis of NIK, p-I $\kappa$ B $\alpha$  (Ser32/36) and tubulin as a loading control in HUVECs transduced with adenoviral vectors expressing GFP (AdGFP) or wild-type NIK (AdNIK-WT) at 250 MOIs, followed by treatment with DMSO or IKK $\beta$ i (2.5  $\mu$ M) for 16 h. Cells were incubated with the proteasome inhibitor MG132 (50  $\mu$ M) for the final hour to prevent p-I $\kappa$ B $\alpha$  degradation. Left panel: immunoblotting data from a representative experiment. Right panel: densitometric analysis of p-I $\kappa$ B $\alpha$  bands from four independent experiments. (G) Real-time qPCR quantification of the *CXCL5*, *GM-CSF*, *CCL5*, *ICAM-1*, *VCAM-1* and E-selectin transcripts expressed in HUVECs transduced with AdGFP or AdNIK-WT (250 MOIs), followed by treatment with DMSO or IKK $\beta$ i (2.5  $\mu$ M) for 16 h. Data represent mean $\pm$ s.e.m. of three (B,D,E,G) or four (A,C,F) independent experiments. ns, not significant; \* $P$ ≤0.05, \*\* $P$ ≤0.01 [one-way ANOVA and Tukey's HSD post hoc test (A–E) or Student's *t*-test (F,G)].

in MCDB131 medium supplemented with 2% v/v FBS. In experiments with IKK $\beta$  and NIK inhibitors, HUVECs were treated with inhibitors for 30 min prior to stimulation with LT $\beta$ . On the day of the assay, Jurkat cells, THP-1 cells and neutrophils were washed with PBS and fluorescently stained with calcein-AM. After 30 min incubation at 37°C, calcein-labeled leukocytes were washed twice with serum-free RPMI-1640 medium and added to ECs in a 96-well plate. After 30–40 min incubation at 37°C, non-adherent

calcein-labeled cells were extensively washed away with serum-free RPMI-1640 medium. Subsequently, fluorescence was measured with the Tecan SpectraFluor fluorescence plate reader using 485/530 nm excitation/emission filter sets. Each condition was tested in quadruplicates. Photos of calcein-labeled leukocytes attached to ECs were taken with a fluorescence microscope equipped with a 10 $\times$  objective and a camera (Nikon Eclipse TE2000-S).

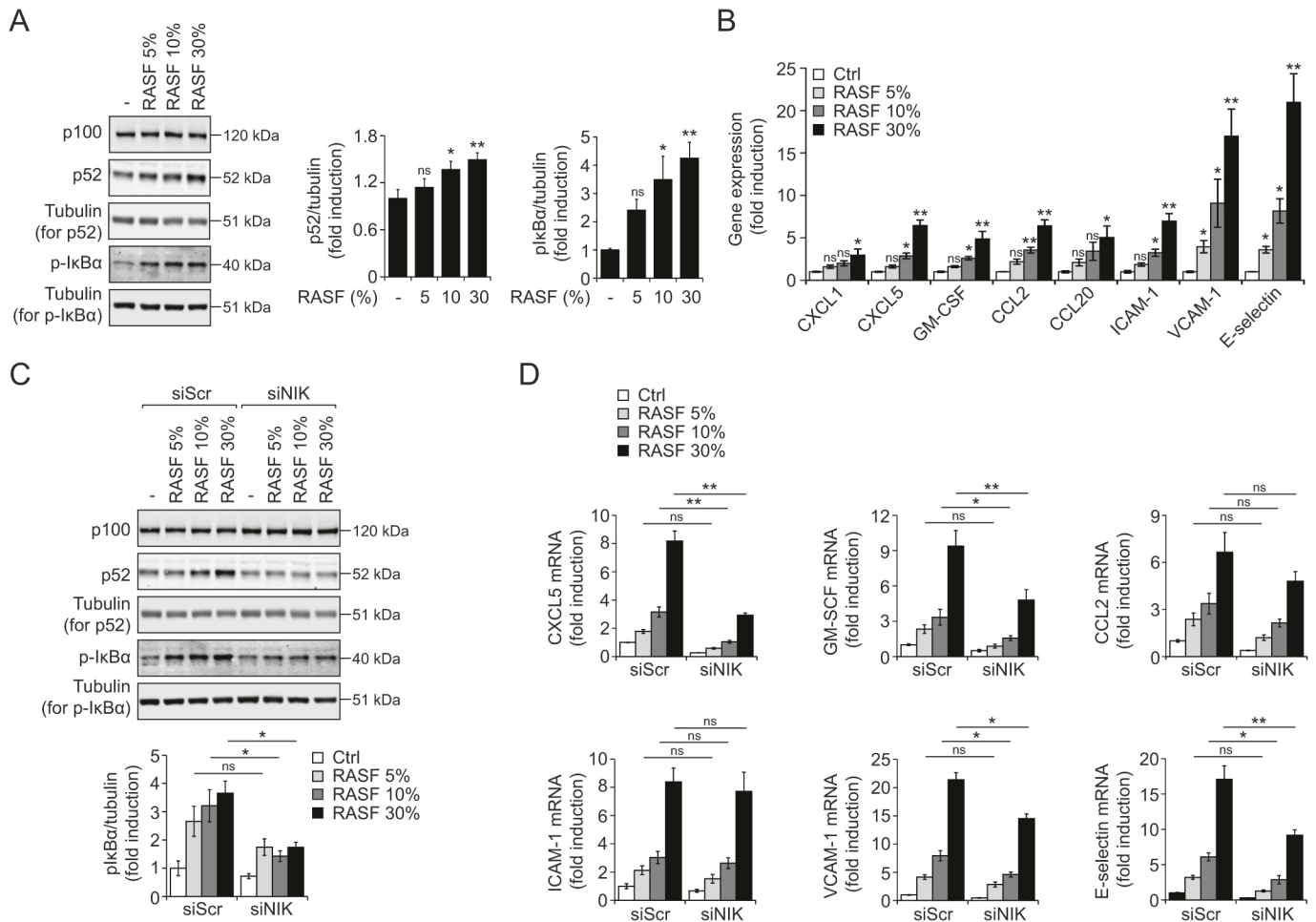


**Fig. 7. NIK regulates RASf-mediated inflammatory activation of ECs.** (A) Immunoblot analysis of p100/p52, p-IkBa $\alpha$  (Ser32/36) and tubulin as a loading control in HUVECs stimulated with RASf at the indicated concentrations for 3 h (p-IkBa $\alpha$  detection) or 6 h (p52 detection). Cells were incubated with the proteasome inhibitor MG132 (50  $\mu$ M) for the final hour to prevent p-IkBa $\alpha$  degradation. Left panel: immunoblotting data from a representative RASf pool. Middle and right panels: densitometric analysis of p52 and p-IkBa $\alpha$  bands from four independent RASf pools. (B) Real-time qPCR quantification of the *CXCL1*, *CXCL5*, *GM-CSF*, *CCL2*, *CCL20*, *ICAM-1*, *VCAM-1* and E-selectin transcripts expressed in HUVECs stimulated with RASf at the indicated concentrations for 6 h. (C) Immunoblot analysis of p100/p52, p-IkBa $\alpha$  (Ser32/36) and tubulin as a loading control in HUVECs transfected with scrambled siRNA (siScr; 10 nM) or siRNA targeting NIK (siNIK; 10 nM) and stimulated with RASf at the indicated concentrations for 3 h (p-IkBa $\alpha$  detection) or 6 h (p52 detection). Cells were incubated with the proteasome inhibitor MG132 (50  $\mu$ M) for the final hour to prevent p-IkBa $\alpha$  degradation. Upper panel: immunoblotting data from a representative RASf pool. Lower panel: densitometric analysis of p-IkBa $\alpha$  bands from four independent RASf pools. (D) Real-time qPCR quantification of the *CXCL5*, *GM-CSF*, *CCL2*, *ICAM-1*, *VCAM-1* and E-selectin transcripts expressed in HUVECs transfected with siScr or siNIK as in C, and stimulated with RASf at the indicated concentrations for 6 h. Data represent mean  $\pm$  s.e.m. of four independent RASf pools. ns, not significant; \* $P$   $\leq$  0.05, \*\* $P$   $\leq$  0.01 versus control (one-way ANOVA and Tukey's HSD post hoc test).

### Endothelial permeability assay

Permeability across EC monolayers was measured using fibronectin-coated Transwell units (6.5 mm diameter, 0.4  $\mu$ m pore size polycarbonate filter; Corning Costar). ECs were plated at density of  $1.2 \times 10^5$  cells per Transwell unit (upper chamber) and cultured for 4 days until the formation of a tight monolayer. Cells were then washed with serum-free MCDB131 medium and stimulated for 24 h with LT $\beta$  or TNF $\alpha$  in complete MCDB131 medium. EC permeability was determined by measuring the passage of FITC-conjugated 10 kDa dextran (1 mg/ml) through the EC monolayer. After 30 min of treatment, the amount of FITC-dextran diffused into the bottom chamber was evaluated by measuring the fluorescence in the medium collected from the lower compartment with the Tecan SpectraFluor fluorescence plate reader using 485/530 nm excitation/emission filter sets. Each condition was tested in quadruplicates.

### RNA interference

ECs were transfected with siRNAs using Lipofectamine<sup>TM</sup> RNAiMAX Transfection Reagent (Thermo Fisher Scientific) as recommended by the

manufacturer. The following siRNAs were used: NIK siRNA (Stealth siRNA, id: HSS113310, Invitrogen), NIK siRNA-2 (Silencer Select, id: s17188, Invitrogen), p100 siRNAs (Stealth siRNA, id: HSS107146 and HSS107147, Invitrogen), IKK $\alpha$  siRNAs (Stealth siRNA, id: HSS101936 and HSS101937, Invitrogen), IKK $\beta$  siRNA (siGENOME SMARTpool, M-003503-03-0005, Dharmacon), scrambled siRNAs [Stealth RNAi<sup>TM</sup> siRNA Negative Control Lo GC Duplex #3, Invitrogen (control for siNIK, sip100 and siIKK $\alpha$ ); Silencer Select Negative Control No. 1 siRNA (control for siNIK-2); siControl Non-targeting siRNA pool, D-001206-13-20, Dharmacon (control for siIKK $\beta$ )]. After 5 h of transfection, ECs were washed twice with PBS and incubated with complete MCDB131 medium for 1–2 days prior to further analysis.

### LDH viability assay

Toxicity of NIK inhibitor was assessed using an In Vitro Toxicology Assay Kit (Sigma-Aldrich), which measures the plasma membrane integrity as a function of the amount of cytoplasmic lactate dehydrogenase (LDH) released into the medium. Cells were incubated in medium containing 0.1, 1

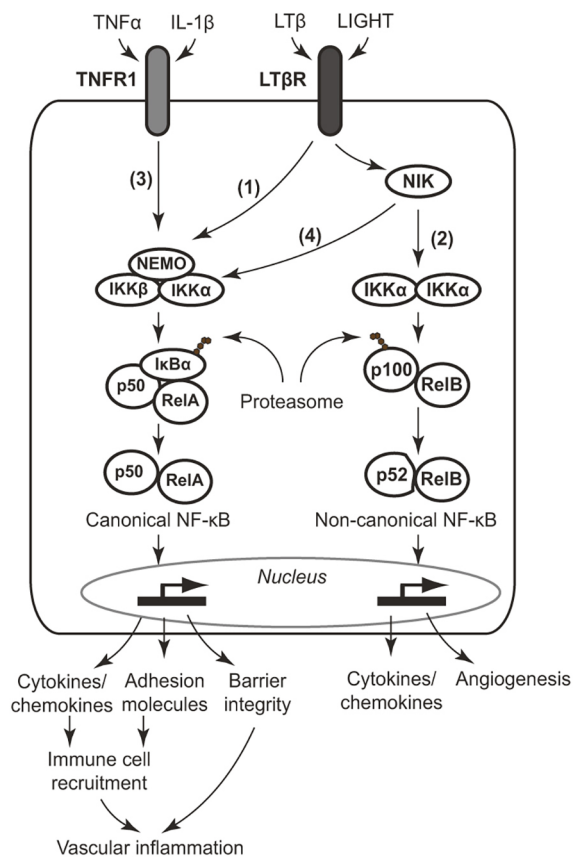


**Fig. 8. Schematic model of LTβR ligation-induced inflammatory signaling in vascular ECs.** LTβR ligation is driven by two major ligands, LTβ and LIGHT, and results in activation of both canonical (1) and non-canonical (2) NF-κB signaling pathways, distinguishing it from pro-inflammatory cytokines, such as TNFα and IL-1β, that only induce the canonical mechanism (3). Long-term ligation of LTβR in ECs, leading to accumulation of NIK, drives angiogenesis and cytokine/chemokine secretion via the non-canonical NF-κB pathway (Noort et al., 2014), as well as vascular inflammation via activation of the IKK complex in an NIK- and IKKα-dependent manner (4). Consequently, in addition to regulating non-canonical signaling, NIK can serve as an amplifier of canonical NF-κB signaling and associated inflammatory responses in ECs, which may play a role in development and maintenance of chronic inflammation.

or 10 μM NIK inhibitor or DMSO for 24 h or 48 h. Hereafter, medium was removed and the LDH activity was assayed according to the protocol provided by the manufacturer. All samples were measured in triplicates.

#### MTT viability assay

Toxicity of IKKβ inhibitor was assessed using MTT assay. Cells were incubated in medium containing 0.1, 1, 2.5, 5 or 10 μM IKKβ inhibitor or DMSO for 24 h or 48 h. Hereafter, medium was replaced by medium containing 1 mg/ml MTT (Sigma-Aldrich). After 2 h, medium was removed from wells and the reaction product, formazan, was solubilized using acidified isopropanol (4 mM HCl, 0.1% Igepal CA630, Sigma-Aldrich) and absorbance was measured at 595 nm. All samples were measured in triplicates.

#### Transduction with adenoviral vectors

Adenoviral vectors encoding GFP (AdGFP), wild-type NIK (AdNIK-WT) and kinase-dead NIK (AdNIK-KD) were kindly provided by Prof. D. Wallach, Weizmann Institute of Science, Israel (Ramakrishnan et al., 2004). Cells were transduced with vectors at various MOIs (indicated in the figure legends) in complete MCDB131 medium for 24 h, and then used for further analysis.

#### Statistical analysis

Statistical significance was evaluated with Student's two-tailed unpaired *t*-test (two groups) or one-way ANOVA and Tukey's HSD post hoc test (>2 groups). Significance of mean comparison is annotated as follows: ns, non-significant ( $P > 0.05$ ); \* $P \leq 0.05$  and \*\* $P \leq 0.01$ .

#### Competing interests

P.K., E.I., M.F. and H.K.O. are employees of AstraZeneca, which supported the study. C.X.M., K.C.M.J., J.P.v.H. and S.W.T. declare no conflicts of interest.

#### Author contributions

Conceptualization: P.K., S.W.T., H.K.O.; Methodology: P.K., C.X.M., K.C.M.J., J.P.v.H., E.I.; Formal analysis: P.K., C.X.M., K.C.M.J., J.P.v.H., E.I.; Investigation: P.K., C.X.M., K.C.M.J.; Resources: M.F., S.W.T.; Data curation: P.K.; Writing - original draft: P.K., H.K.O.; Writing - review & editing: P.K., C.X.M., K.C.M.J., J.P.v.H., E.I., M.F., S.W.T., H.K.O.; Supervision: S.W.T., H.K.O.; Project administration: H.K.O.; Funding acquisition: H.K.O.

#### Funding

This study was supported by the internal AstraZeneca postdoc program [P.K.], and research grants from Reumafonds [13-3-304; 2016-1-032 to S.W.T., J.P.v.H. and K.C.M.J.] and Academisch Medisch Centrum/Universiteit van Amsterdam [C.X.M.].

#### Supplementary information

Supplementary information available online at <http://jcs.biologists.org/lookup/doi/10.1242/jcs.225615.supplemental>

#### References

- Adli, M., Merkhofer, E., Cogswell, P. and Baldwin, A. S. (2010). IKKalpha and IKKbeta each function to regulate NF-kappaB activation in the TNF-induced/canonical pathway. *PLoS ONE* **5**, e9428.
- Al-Soudi, A., Kaaij, M. H. and Tas, S. W. (2017). Endothelial cells: From innocent bystanders to active participants in immune responses. *Autoimmun. Rev.* **16**, 951-962.
- Andersson, P., Börjesson, L., Eriksson, C. and Larsson, J. (2008). A pharmaceutical composition comprising an ikk2 inhibitor and a second active ingredient. Google Patents (WO 2008002246 A1).
- Anest, V., Hanson, J. L., Cogswell, P. C., Steinbrecher, K. A., Strahl, B. D. and Baldwin, A. S. (2003). A nucleosomal function for IkkappaB kinase-alpha in NF-kappaB-dependent gene expression. *Nature* **423**, 659-663.
- Aya, K., Alhawagri, M., Hagen-Stapleton, A., Kitaura, H., Kanagawa, O. and Veis Novack, D. (2005). NF-(kappa)B-inducing kinase controls lymphocyte and osteoclast activities in inflammatory arthritis. *J. Clin. Invest.* **115**, 1848-1854.
- Bonizzi, G., Bebie, M., Otero, D. C., Johnson-Vroom, K. E., Cao, Y., Vu, D., Jegga, A. G., Aronow, B. J., Ghosh, G., Rickett, R. C. et al. (2004). Activation of IKKalpha target genes depends on recognition of specific kappaB binding sites by RelB:p52 dimers. *EMBO J.* **23**, 4202-4210.
- Chang, Y. H., Hsieh, S. L., Chao, Y., Chou, Y. C. and Lin, W. W. (2005). Proinflammatory effects of LIGHT through HVEM and LTbetaR interactions in cultured human umbilical vein endothelial cells. *J. Biomed. Sci.* **12**, 363-375.
- Dejardin, E., Droin, N. M., Delhase, M., Haas, E., Cao, Y., Makris, C., Li, Z.-W., Karin, M., Ware, C. F. and Green, D. R. (2002). The lymphotoxin-beta receptor induces different patterns of gene expression via two NF-kappaB pathways. *Immunity* **17**, 525-535.
- De Martin, R., Hoeth, M., Hofer-Warbinek, R. and Schmid, J. A. (2000). The transcription factor NF-kappa B and the regulation of vascular cell function. *Arterioscler. Thromb. Vasc. Biol.* **20**, E83-E88.
- Eishabrawy, H. A., Chen, Z., Volin, M. V., Ravello, S., Virupannavar, S. and Shahrara, S. (2015). The pathogenic role of angiogenesis in rheumatoid arthritis. *Angiogenesis* **18**, 433-448.
- Hayden, M. S. and Ghosh, S. (2004). Signaling to NF-kappaB. *Genes Dev.* **18**, 2195-2224.
- Hollenbaugh, D., Mischel-Petty, N., Edwards, C. P., Simon, J. C., Denfeld, R. W., Kiener, P. A. and Aruffo, A. (1995). Expression of functional CD40 by vascular endothelial cells. *J. Exp. Med.* **182**, 33-40.
- Hu, Y., Baud, V., Delhase, M., Zhang, P., Deerinck, T., Ellisman, M., Johnson, R. and Karin, M. (1999). Abnormal morphogenesis but intact IKK activation in mice lacking the IKKalpha subunit of IkkappaB kinase. *Science* **284**, 316-320.
- Huang, S., Robinson, J. B., Deguzman, A., Bucana, C. D. and Fidler, I. J. (2000). Blockade of nuclear factor-kappaB signaling inhibits angiogenesis and tumorigenicity of human ovarian cancer cells by suppressing expression of vascular endothelial growth factor and interleukin 8. *Cancer Res.* **60**, 5334-5339.
- Humby, F., Bombardieri, M., Manzo, A., Kelly, S., Blades, M. C., Kirkham, B., Spencer, J. and Pitzalis, C. (2009). Ectopic lymphoid structures support ongoing production of class-switched autoantibodies in rheumatoid synovium. *PLoS Med.* **6**, e1.

- Hynd, G., Price, S., Kulagowski, J., Macleod, C., Mann, S. E., Panchal, T. A., Tisselli, P. and Montana, J. G. (2014). 3-(2-aminopyrimidin-4-yl)-5-(3-hydroxypropyl)-1H-pyrrolo[2,3-c]pyridine derivatives as NIK inhibitors for the treatment of cancer. Google Patents (WO 2014174021 A1).
- Jones, G. W. and Jones, S. A. (2016). Ectopic lymphoid follicles: inducible centres for generating antigen-specific immune responses within tissues. *Immunology* **147**, 141-151.
- Kempe, S., Kestler, H., Lasar, A. and Wirth, T. (2005). NF-kappaB controls the global pro-inflammatory response in endothelial cells: evidence for the regulation of a pro-atherogenic program. *Nucleic Acids Res.* **33**, 5308-5319.
- Kew, R. R., Penzo, M., Habieli, D. M. and Marcu, K. B. (2012). The IKK $\alpha$ -dependent NF- $\kappa$ B p52/RelB noncanonical pathway is essential to sustain a CXCL12 autocrine loop in cells migrating in response to HMGB1. *J. Immunol.* **188**, 2380-2386.
- Kraan, M. C., Reece, R. J., Smeets, T. J. M., Veale, D. J., Emery, P. and Tak, P. P. (2002). Comparison of synovial tissues from the knee joints and the small joints of rheumatoid arthritis patients: Implications for pathogenesis and evaluation of treatment. *Arthritis. Rheum.* **46**, 2034-2038.
- Lau, T.-S., Chung, T. K.-H., Cheung, T.-H., Chan, L. K.-Y., Cheung, L. W.-H., Yim, S.-F., Siu, N. S.-S., Lo, K.-W., Yu, M. M.-Y., Kulbe, H. et al. (2014). Cancer cell-derived lymphotoxin mediates reciprocal tumour-stromal interactions in human ovarian cancer by inducing CXCL11 in fibroblasts. *J. Pathol.* **232**, 43-56.
- Lee, H., Herrmann, A., Deng, J. H., Kujawski, M., Niu, G., Li, Z., Forman, S., Jove, R., Pardoll, D. M. and Yu, H. (2009). Persistently activated Stat3 maintains constitutive NF-kappa B activity in tumors. *Cancer Cell* **15**, 283-293.
- Li, J., Peet, G. W., Pullen, S. S., Schembri-King, J., Warren, T. C., Marcu, K. B., Kehry, M. R., Barton, R. and Jakes, S. (1998). Recombinant IkappaB kinases alpha and beta are direct kinases of Ikappa Balpha. *J. Biol. Chem.* **273**, 30736-30741.
- Li, Q., Lu, Q., Hwang, J. Y., Büscher, D., Lee, K.-F., Izipisua-Belmonte, J. C. and Verma, I. M. (1999). IKK1-deficient mice exhibit abnormal development of skin and skeleton. *Genes Dev.* **13**, 1322-1328.
- Ling, L., Cao, Z. and Goeddel, D. V. (1998). NF-kappaB-inducing kinase activates IKK-alpha by phosphorylation of Ser-176. *Proc. Natl. Acad. Sci. USA* **95**, 3792-3797.
- Lovas, A., Radke, D., Albrecht, D., Yilmaz, Z. B., Möller, U., Habenicht, A. J. R. and Weih, F. (2008). Differential RelA- and RelB-dependent gene transcription in LTbetaR-stimulated mouse embryonic fibroblasts. *BMC Genomics* **9**, 606.
- Madge, L. A., Kluger, M. S., Orange, J. S. and May, M. J. (2008). Lymphotoxin-alpha 1 beta 2 and LIGHT induce classical and noncanonical NF-kappa B-dependent proinflammatory gene expression in vascular endothelial cells. *J. Immunol.* **180**, 3467-3477.
- Maijer, K. I., Noort, A. R., de Hair, M. J. H., van der Leij, C., van Zoest, K. P. M., Choi, I. Y., Gerlag, D. M., Maas, M., Tak, P. P. and Tas, S. W. (2015). Nuclear Factor-kappaB-inducing kinase is expressed in synovial endothelial cells in patients with early arthritis and correlates with markers of inflammation: a prospective cohort study. *J. Rheumatol.* **42**, 1573-1581.
- Maracle, C. X., Kucharzewska, P., Helder, B., van der Horst, C., Correa de Sampaio, P., Noort, A.-R., van Zoest, K., Griffioen, A. W., Olsson, H. and Tas, S. W. (2017). Targeting non-canonical nuclear factor-kappaB signalling attenuates neovascularization in a novel 3D model of rheumatoid arthritis synovial angiogenesis. *Rheumatology* **56**, 294-302.
- Matsushima, A., Kaisho, T., Rennert, P. D., Nakano, H., Kurosawa, K., Uchida, D., Takeda, K., Akira, S. and Matsumoto, M. (2001). Essential role of nuclear factor (NF)-kappaB-inducing kinase and inhibitor of kappaB (IkappaB) kinase alpha in NF-kappaB activation through lymphotoxin beta receptor, but not through tumor necrosis factor receptor I. *J. Exp. Med.* **193**, 631-636.
- Müller, J. R. and Siebenlist, U. (2003). Lymphotoxin beta receptor induces sequential activation of distinct NF-kappa B factors via separate signaling pathways. *J. Biol. Chem.* **278**, 12006-12012.
- Murdaca, G., Colombo, B. M., Cagnati, P., Gulli, R., Spanò, F. and Puppo, F. (2012). Endothelial dysfunction in rheumatic autoimmune diseases. *Atherosclerosis* **224**, 309-317.
- Nadiminty, N., Chun, J. Y., Hu, Y., Dutt, S., Lin, X. and Gao, A. C. (2007). LIGHT, a member of the TNF superfamily, activates Stat3 mediated by NIK pathway. *Biochem. Biophys. Res. Commun.* **359**, 379-384.
- Napetschnig, J. and Wu, H. (2013). Molecular basis of NF-kappaB signaling. *Annu. Rev. Biophys.* **42**, 443-468.
- Noort, A. R., van Zoest, K. P. M., Weijers, E. M., Koolwijk, P., Maracle, C. X., Novack, D. V., Siemerink, M. J., Schlingemann, R. O., Tak, P. P. and Tas, S. W. (2014). NF-kappaB-inducing kinase is a key regulator of inflammation-induced and tumour-associated angiogenesis. *J. Pathol.* **234**, 375-385.
- Noort, A. R., van Zoest, K. P., van Baarsen, L. G., Maracle, C. X., Helder, B., Papazian, N., Romera-Hernandez, M., Tak, P. P., Cupedo, T. and Tas, S. W. (2015a). Tertiary lymphoid structures in rheumatoid arthritis: NF-kappaB-Inducing kinase-positive endothelial cells as central players. *Am. J. Pathol.* **185**, 1935-1943.
- Noort, A. R., Tak, P. P. and Tas, S. W. (2015b). Non-canonical NF-kappaB signaling in rheumatoid arthritis: Dr Jekyll and Mr Hyde? *Arthritis Res. Ther.* **17**, 15.
- Novack, D. V., Yin, L., Hagen-Stapleton, A., Schreiber, R. D., Goeddel, D. V., Ross, F. P. and Teitelbaum, S. L. (2003). The IkappaB function of NF-kappaB2 p100 controls stimulated osteoclastogenesis. *J. Exp. Med.* **198**, 771-781.
- O'Mahony, A., Lin, X., Gelezianus, R. and Greene, W. C. (2000). Activation of the heterodimeric IKKalpha-IKKbeta complex is directional: IKKalpha regulates IKKbeta under both basal and stimulated conditions. *Mol. Cell. Biol.* **20**, 1170-1178.
- Onder, L., Danuser, R., Scandella, E., Firner, S., Chai, Q., Hehlgans, T., Stein, J. V. and Ludewig, B. (2013). Endothelial cell-specific lymphotoxin-beta receptor signaling is critical for lymph node and high endothelial venule formation. *J. Exp. Med.* **210**, 465-473.
- Park, G. Y., Wang, X., Hu, N., Pedchenko, T. V., Blackwell, T. S. and Christman, J. W. (2006). NIK is involved in nucleosomal regulation by enhancing histone H3 phosphorylation by IKKalpha. *J. Biol. Chem.* **281**, 18684-18690.
- Pitzalis, C., Jones, G. W., Bombardieri, M. and Jones, S. A. (2014). Ectopic lymphoid-like structures in infection, cancer and autoimmunity. *Nat. Rev. Immunol.* **14**, 447-462.
- Pober, J. S. and Sessa, W. C. (2007). Evolving functions of endothelial cells in inflammation. *Nat. Rev. Immunol.* **10**, 803-815.
- Ramakrishnan, P., Wang, W. and Wallach, D. (2004). Receptor-specific signaling for both the alternative and the canonical NF-kappaB activation pathways by NF-kappaB-inducing kinase. *Immunity* **21**, 477-489.
- Scheinman, R. I., Beg, A. A. and Baldwin, A. S. Jr (1993). NF-kappa B p100 (Lyt-10) is a component of H2TF1 and can function as an I kappa B-like molecule. *Mol. Cell. Biol.* **13**, 6089-6101.
- Seigner, J., Basilio, J., Resch, U. and de Martin, R. (2018). CD40L and TNF both activate the classical NF-kappaB pathway, which is not required for the CD40L induced alternative pathway in endothelial cells. *Biochem. Biophys. Res. Commun.* **495**, 1389-1394.
- Smith, C., Andreacos, E., Crawley, J. B., Brennan, F. M., Feldmann, M. and Foxwell, B. M. J. (2001). NF-kappaB-Inducing Kinase is dispensable for activation of NF-kappaB in inflammatory settings but essential for lymphotoxin beta receptor activation of NF-kappaB in primary human fibroblasts. *J. Immunol.* **167**, 5895-5903.
- Steyers, C. M. and Miller, F. J. Jr (2014). Endothelial dysfunction in chronic inflammatory diseases. *Int. J. Mol. Sci.* **15**, 11324-11349.
- Sun, S.-C. (2017). The non-canonical NF-kappaB pathway in immunity and inflammation. *Nat. Rev. Immunol.* **17**, 545-558.
- Tanaka, M., Fuentes, M. E., Yamaguchi, K., Durnin, M. H., Dalrymple, S. A., Hardy, K. L. and Goeddel, D. V. (1999). Embryonic lethality, liver degeneration, and impaired NF-kappaB activation in IKKb-deficient mice. *Immunity* **10**, 421-429.
- Tas, S. W., Maracle, C. X., Balogh, E. and Szekanecz, Z. (2016). Targeting of proangiogenic signalling pathways in chronic inflammation. *Nat. Rev. Rheumatol.* **12**, 111-122.
- Wolf, M. J., Seleznik, G. M., Zeller, N. and Heikenwalder, M. (2010). The unexpected role of lymphotoxin beta receptor signaling in carcinogenesis: from lymphoid tissue formation to liver and prostate cancer development. *Oncogene* **29**, 5006-5018.
- Woronicz, J. D., Gao, X., Cao, Z., Rothe, M. and Goeddel, D. V. (1997). IkappaB kinase-beta: NF-kappaB activation and complex formation with IkappaB kinase-alpha and NIK. *Science* **278**, 866-869.
- Xiao, G., Harhaj, E. W. and Sun, S.-C. (2001). NF-kappaB-inducing kinase regulates the processing of NF-kappaB2 p100. *Mol. Cell.* **7**, 401-409.
- Yamamoto, Y., Yin, M.-J. and Gaynor, R. B. (2000). IKKalpha regulation of IKKbeta kinase activity. *Mol. Cell. Biol.* **20**, 3655-3666.
- Yamamoto, Y., Verma, U. N., Prajapati, S., Kwak, Y.-T. and Gaynor, R. B. (2003). Histone H3 phosphorylation by IKK-alpha is critical for cytokine-induced gene expression. *Nature* **423**, 655-659.
- Yin, L., Wu, L., Wesche, H., Arthur, C. D., White, J. M., Goeddel, D. V. and Schreiber, R. D. (2001). Defective lymphotoxin-beta receptor-induced NF-kappaB transcriptional activity in NIK-deficient mice. *Science* **291**, 2162-2165.
- Yoon, S., Woo, S. U., Kang, J. H., Kim, K., Shin, H.-J., Gwak, H.-S., Park, S. and Chwaee, Y.-J. (2012). NF-kappaB and STAT3 cooperatively induce IL6 in starved cancer cells. *Oncogene* **31**, 3467-3481.
- Yu, J., Wang, Y., Yan, F., Zhang, P., Li, H., Zhao, H., Yan, C., Yan, F. and Ren, X. (2014). Noncanonical NF-kappaB activation mediates STAT3-stimulated IDO upregulation in myeloid-derived suppressor cells in breast cancer. *J. Immunol.* **193**, 2574-2586.
- Zarnegar, B., Yamazaki, S., He, J. Q. and Cheng, G. (2008). Control of canonical NF-kappaB activation through the NIK-IKK complex pathway. *Proc. Natl. Acad. Sci. USA* **105**, 3503-3508.